The Astronomical Journal, 126:742–761, 2003 August

AN ATLAS OF *HUBBLE SPACE TELESCOPE* SPECTRA AND IMAGES OF NEARBY SPIRAL GALAXIES[1]

M. A. Hughes,[2] A. Alonso-Herrero,[3] D. Axon,[2,4] C. Scarlata,[5] J. Atkinson,[2] D. Batcheldor,[2] J. Binney,[6] A. Capetti,[7] C. M. Carollo,[8] L. Dressel,[5] J. Gerssen,[5] D. Macchetto,[5] W. Maciejewski,[9,10] A. Marconi,[9] M. Merrifield,[11] M. Ruiz,[2] W. Sparks,[5] M. Stiavelli,[5] Z. Tsvetanov,[12] and R. van der Marel[5]
Received 2003 April 17; accepted 2003 May 6

ABSTRACT

We have observed 54 nearby spiral galaxies with the Space Telescope Imaging Spectrograph (STIS) on the *Hubble Space Telescope* to obtain optical long-slit spectra of nuclear gas disks and STIS optical ($\sim R$ band) images of the central $5'' \times 5''$ of the galaxies. These spectra are being used to determine the velocity field of nuclear disks and hence to detect the presence of central massive black holes. Here we present the spectra for the successful observations. Dust obscuration can be significant at optical wavelengths, and so we also combine the STIS images with archival Near-Infrared Camera and Multi-Object Spectrometer H-band images to produce color maps to investigate the morphology of gas and dust in the central regions. We find a great variety in the different morphologies, from smooth distributions to well-defined nuclear spirals and dust lanes.

Key words: galaxies: nuclei — galaxies: spiral

1. INTRODUCTION

The field of massive black hole (MBH) astrophysics has expanded greatly in recent years because of the increase in resolution now available through the *Hubble Space Telescope* (*HST*) and adaptive optics–assisted ground-based observations. Multiple searches have indicated that MBHs are present at the centers of many galaxies (e.g., Macchetto et al. 1997; Barth et al. 2001; Schödel et al. 2002). The ultimate aim of these searches is to put the formation and growth of MBHs firmly within the context of galaxy evolution. To assist with this goal several authors have searched for correlations between the mass of the black hole and more general properties of the galaxy such as bulge mass and luminosity (e.g., Kormendy & Richstone 1995; Marconi & Hunt 2003), the stellar velocity dispersion in the bulge (Ferrarese & Merritt 2000; Gebhardt et al. 2000), the luminosity concentration in the central regions (Graham et al. 2001), and the shape of the bulge surface brightness profiles (Graham et al. 2002). Such correlations indicate that the histories of the MBH and host galaxy are interrelated. However, for the region where $M_{\rm BH} \leq 10^7\ M_\odot$, which is expected to be occupied by spiral galaxies, all of the correlations suffer from a lack of directly determined MBH masses.

As a first step to understanding the MBH–host galaxy relationship, we need to establish the mass distribution of MBHs over a wide range of galaxy types. To date, most MBH masses have been determined in massive elliptical galaxies. In their Figure 2, Merritt & Ferrarese (2001) present their correlation between MBH mass and stellar velocity dispersion using only those estimates that they considered to be secure. The number of points for spiral galaxies is small. The current correlations suggest that spiral galaxies will have lower mass MBHs than elliptical galaxies, and so it is crucial that we populate the correlation with good dynamical estimates of MBH masses for spirals. To this end we have undertaken an *HST* Space Telescope Imaging Spectrograph (STIS) program to determine MBH masses for a sample of nearby emission-line spiral galaxies.

This paper is part of a series reporting the results of our *HST* program. In Paper I (Marconi et al. 2003) we report the modeling of the central mass concentration in NGC 4041, the first galaxy to be observed as part of the program. Paper I also contains a detailed description of the modeling techniques that we use to determine MBH masses. In Paper II (this paper) we present the STIS spectra and also create color maps from the optical STIS images when archival Near-Infrared Camera and Multi-Object Spectrometer (NICMOS) images are available. In Paper III (Hughes et al. 2003) we use both color information from these images and the spectra presented here to investigate the age of the central stellar populations. In Paper IV (Scarlata et al. 2003) we present the STIS images acquired in the program and analyze surface brightness profiles derived from the images.

[1] Based on observations with the NASA/ESA *Hubble Space Telescope* obtained at the Space Telescope Science Institute, which is operated by the Association of Universities for Research in Astronomy, Inc., under NASA contract NAS5-26555.

[2] Department of Physical Sciences, University of Hertfordshire, Hatfield, Hertfordshire AL10 9AB, UK.

[3] Steward Observatory, University of Arizona, 933 North Cherry Avenue, Tucson, AZ 85721.

[4] Department of Physics, Rochester Institute of Technology, 84 Lomb Memorial Drive, Rochester, NY 14623-5603.

[5] Space Telescope Science Institute, 3700 San Martin Drive, Baltimore, MD 21218.

[6] Oxford University, Theoretical Physics, Keble Road, Oxford OX1 3NP, UK.

[7] INAF-Osservatorio Astronomico di Torino, I-10025 Pino Torinese, Italy.

[8] Eidgenoessische Technische Hochshule Zürich, Hönggerberg HPF G4.3, CH-8092 Zürich, Switzerland.

[9] INAF-Osservatorio Astrofisico di Arcetri, Largo E. Fermi 5, 50125 Firenze, Italy.

[10] Obserwatorium Astonomiczne Uniwersytetu Jagiellońskiego, Poland.

[11] School of Physics and Astronomy, University of Nottingham, NG7 2RD, UK.

[12] Center for Astrophysical Sciences, Johns Hopkins University, 239 Bloomberg Center for Physics and Astronomy, 3400 North Charles Street, Baltimore, MD 21218.

TABLE 1

The Sample of 54 Nearby Spiral Galaxies

Galaxy	N?	Morphology	Nuclear Activity	Date Observed	Recessional Velocity (km s^{-1})	NUC Slit (arcsec)	NUC Bin.	Spectra Quality
NGC 0134.......	No	SAB(s)bc	. . . (. . .)	2000 Jul 7	1399	52 × 0.2	1 × 1	Missed galaxy center
NGC 0157.......	Yes	SAB(rs)bc	. . . (. . .)	1999 Nov 3	1589	52 × 0.1	1 × 1	Dust obscures center
NGC 0255.......	No	SAB(rs)bc	. . . (. . .)	1999 Oct 26	1502	52 × 0.1	1 × 1	None
NGC 0289.......	Yes	SAB(rs)bc	. . . (. . .)	2000 Oct 25	1451	52 × 0.2	1 × 1	Weak cont., motion
NGC 0613.......	No	SB(rs)bc Sy	. . . (. . .)	2000 Sep 22	1302	52 × 0.2	1 × 1	Ext., broad., weak cont., motion
NGC 1255.......	No	SAB(rs)bc	. . . (. . .)	1999 Oct 17	1498	52 × 0.1	1 × 1	Ext., no cont. in OFF 1 and 2
NGC 1300.......	Yes	(R')SB(s)bc	. . . (. . .)	2000 Oct 29	1409	52 × 0.2	1 × 1	Weak cont., ext.
NGC 1832.......	No	SB(r)bc	. . . (. . .)	2000 Jul 22	1782	52 × 0.2	1 × 1	Weak cont., ext., motion
NGC 2748.......	Yes	SAbc	. . . (H)	2000 Nov 9	1741	52 × 0.2	1 × 1	Ext., no cont.
NGC 2903.......	Yes	SB(s)d	H (H)	2000 Feb 3	626	52 × 0.2	2 × 2	Weak cont., motion, ext.
NGC 2964.......	No	SAB(r)bc	H (H)	2000 Oct 4	1446	52 × 0.2	1 × 1	Weak cont., motion, ext.
NGC 3003.......	No	SBbc	. . . (H)	2000 Mar 20	1611	52 × 0.2	2 × 2	Weak cont., ext.
NGC 3021.......	No	SA(rs)bc	. . . (. . .)	2000 Apr 24	1673	52 × 0.2	1 × 1	Ext.
NGC 3162.......	No	SAB(rs)bc	. . . (. . .)	2000 Jan 27	1390	52 × 0.2	2 × 2	Motion, ext.
NGC 3254.......	No	SA(s)bc	S2 (S2)	2000 Dec 5	1478	52 × 0.2	1 × 1	Poor
NGC 3259.......	Yes	SAB(rs)bc	. . . (. . .)	2000 Jul 9	1929	52 × 0.2	1 × 1	Weak cont.
NGC 3310.......	Yes	SAB(r)bc pec	H (H)	2000 Feb 11	1208	52 × 0.2	2 × 2	Motion, ext.
NGC 3403.......	No	SAbc	. . . (. . .)	2000 Oct 30	1528	52 × 0.2	1 × 1	None
NGC 3521.......	No	SAB(rs)b	L (H/L2::)	2000 Mar 3	804	52 × 0.2	2 × 2	None
NGC 3642.......	No	SA(r)bc	L (L1.9)	2000 Oct 13	1831	52 × 0.2	1 × 1	Poor
NGC 3684.......	No	SA(rs)bc	H (H)	2000 Mar 25	1252	52 × 0.2	2 × 2	Poor
NGC 3686.......	No	SB(s)bc	. . . (H)	2001 Feb 17	1245	52 × 0.2	1 × 1	Broad in NUC, no cont. in OFF 1 and 2
NGC 3756.......	No	SAB(rs)bc	. . . (H)	2001 Jan 24	1525	52 × 0.2	1 × 1	Poor
NGC 3887.......	No	SB(r)bc	. . . (H)	2000 Apr 2	1140	52 × 0.2	2 × 2	Weak ext.
NGC 3949.......	Yes	SA(s)bc	H (H)	2000 Apr 4	1021	52 × 0.2	2 × 2	Weak cont. in OFF, ext.
NGC 3953.......	No	SB(r)bc	H/L (. . .)	2000 Feb 11	1287	52 × 0.2	2 × 2	None
NGC 3972.......	No	SA(s)bc	. . . (. . .)	2000 Oct 2	1088	52 × 0.2	1 × 1	None
NGC 4030.......	Yes	SA(s)bc	. . . (. . .)	2000 Feb 20	1475	52 × 0.2	2 × 2	Hα present?
NGC 4041.......	No	SA(rs)bc	. . . (H)	1999 Jul 3	1486	52 × 0.1	1 × 1	Weak cont., ext.
NGC 4051.......	No	SAB(rs)bc	S1.5 (S1.2)	2000 Mar 12	922	52 × 0.2	2 × 2	Broad, weak ext., strong cont. on NUC
NGC 4088.......	No	SAB(rs)bc	. . . (H)	2000 Jul 9	988	52 × 0.2	1 × 1	Weak cont., ext.
NGC 4100.......	No	(R')SA(rs)bc	H (H)	2000 Feb 26	1303	52 × 0.2	2 × 2	Weak cont., ext.
NGC 4212.......	No	SAc	. . . (H)	2000 May 12	9	52 × 0.2	1 × 1	Motion, weak cont., ext.
NGC 4258.......	Yes	SAB(s)bc	L/S1.9 (S1.9)	2000 Aug 1	674	52 × 0.2	1 × 1	Broad, ext.
NGC 4303.......	Yes	SAB(rs)bc	H/S2 (H)	2000 Mar 31	1619	52 × 0.2	2 × 2	Ext.
NGC 4321.......	No	SAB(s)bc	L/H (T2)	2000 May 22	1682	52 × 0.2	1 × 1	Broad, ext.
NGC 4389.......	Yes	SB(rs)bc pec	. . . (. . .)	1999 Oct 26	940	52 × 0.1	1 × 1	Weak cont., ext.
NGC 4420.......	No	SB(r)bc	. . . (. . .)	2000 Mar 18	1730	52 × 0.2	2 × 2	None
NGC 4527.......	Yes	SAB(s)bc	H/L(T2)	1999 Jul 13	1776	52 × 0.1	1 × 1	Poor but some ext.
NGC 4536.......	Yes	SAB(rs)bc	H (H)	2000 Mar 26	1846	52 × 0.2	2 × 2	Ext., motion
NGC 5005.......	Yes	SAB(rs)bc	S2/L (L1.9)	2001 Dec 24	1153	52 × 0.2	1 × 1	Weak cont., broad
NGC 5054.......	Yes	SA(s)bc	. . . (. . .)	2000 Aug 4	1704	52 × 0.2	2 × 2	Weak cont., ext., motion
NGC 5055.......	Yes	SA(rs)bc	H/L (T2)	2000 Apr 16	726	52 × 0.2	2 × 2	Strong cont., motion, ext.
NGC 5247.......	No	SA(s)bc	. . . (. . .)	2000 May 4	1319	52 × 0.2	1 × 1	Poor
NGC 5248.......	Yes	(R) SB(rs)bc	S2/H (H)	2000 Apr 18	1248	52 × 0.2	1 × 1	Ext., second cont. in OFF 2
NGC 5364.......	No	SA(rs)bc pec	H (H)	2000 Mar 5	1322	52 × 0.2	2 × 2	Poor
NGC 5577.......	Yes	SA(rs)bc	. . . (. . .)	2000 Mar 6	1568	52 × 0.2	2 × 2	None
NGC 5713.......	No	SAB(rs)bc pec	H (. . .)	2000 Apr 1	1954	52 × 0.2	2 × 2	Missed galaxy center
NGC 5879.......	Yes	SA(rs)bc?	L (T2/L2)	2000 Mar 12	1049	52 × 0.2	2 × 2	Weak cont., ext.
NGC 5921.......	No	SB(r)bc	L (T2)	2000 May 20	1581	52 × 0.2	1 × 1	Ext.
NGC 6384.......	Yes	SAB(r)bc	L (T2)	2000 Mar 24	1780	52 × 0.2	2 × 2	None
NGC 6951.......	Yes	SAB(rs)bc	L/S2 (S2)	2000 Jun 17	1705	52 × 0.2	1 × 1	Weak cont., broad., ext.
NGC 7314.......	No	SAB(rs)bc	S1.9 (. . .)	2000 Sep 4	1312	52 × 0.2	2 × 2	Broad, weak cont. in OFF 1 and 2
NGC 7331.......	Yes	SA(s)b	L (T2)	2000 Jul 3	992	52 × 0.2	1 × 1	Poor

Notes.—This is the complete sample of galaxies observed during *HST* program 8228. " N? " indicates those galaxies for which nonproprietary *H*-band NICMOS images were available at the time. The morphological classification and activity status are taken from NED, with classification shown in parenthesis taken from Ho, Filippenko, & Sargent 1997, where H = H II nuclei, S = Seyfert nuclei, L = LINER, and T = transition nuclei. Recessional velocities are corrected for Virgo infall (LEDA). " NUC slit " and " OFF slit " refer to the aperture size (in arcseconds) used for the on-nucleus and off-nucleus slit positions, respectively. " NUC Bin." is the on-chip binning strategy for the on-nucleus slit and is either no binning (1 × 1) or 2 × 2 binning. For the OFF 1 and OFF 2 slits the $52'' \times 0''.2$ aperture was used in conjunction with 2 × 2 on-chip binning. Key features of the spectra morphology are summarized as follows: " ext." means some extended emission is present, " cont." refers to the continuum, " broad " indicates some broad lines are present, " motion " means that motion is obvious from wavelength shifts in the emission lines, " none " means the spectra were blank or too faint to use, and " poor " means some evidence of lines or continuum but of poor quality for the MBH program.

2. THE SPECTRA AND IMAGES

Table 1 lists all of the galaxies in our *HST* program (PI: Axon, PID: 8228). The subsample of 23 galaxies with archival NICMOS images is indicated by an " N " in Table 1. The galaxies come from a larger sample of 128 spiral galaxies that show Hα emission on large scales (Axon et al. 2003). Selecting only galaxies with clear emission lines was necessary since we kinematically model the nuclear gas disks, as described in Paper I. All the galaxies are currently classified as late-type spirals and are nearby, having recessional velocities of less than 2000 km s^{-1}. Throughout this paper we assume a Hubble constant of $H_0 = 75$ km s^{-1} Mpc^{-1}, which means that the galaxies of the sample are

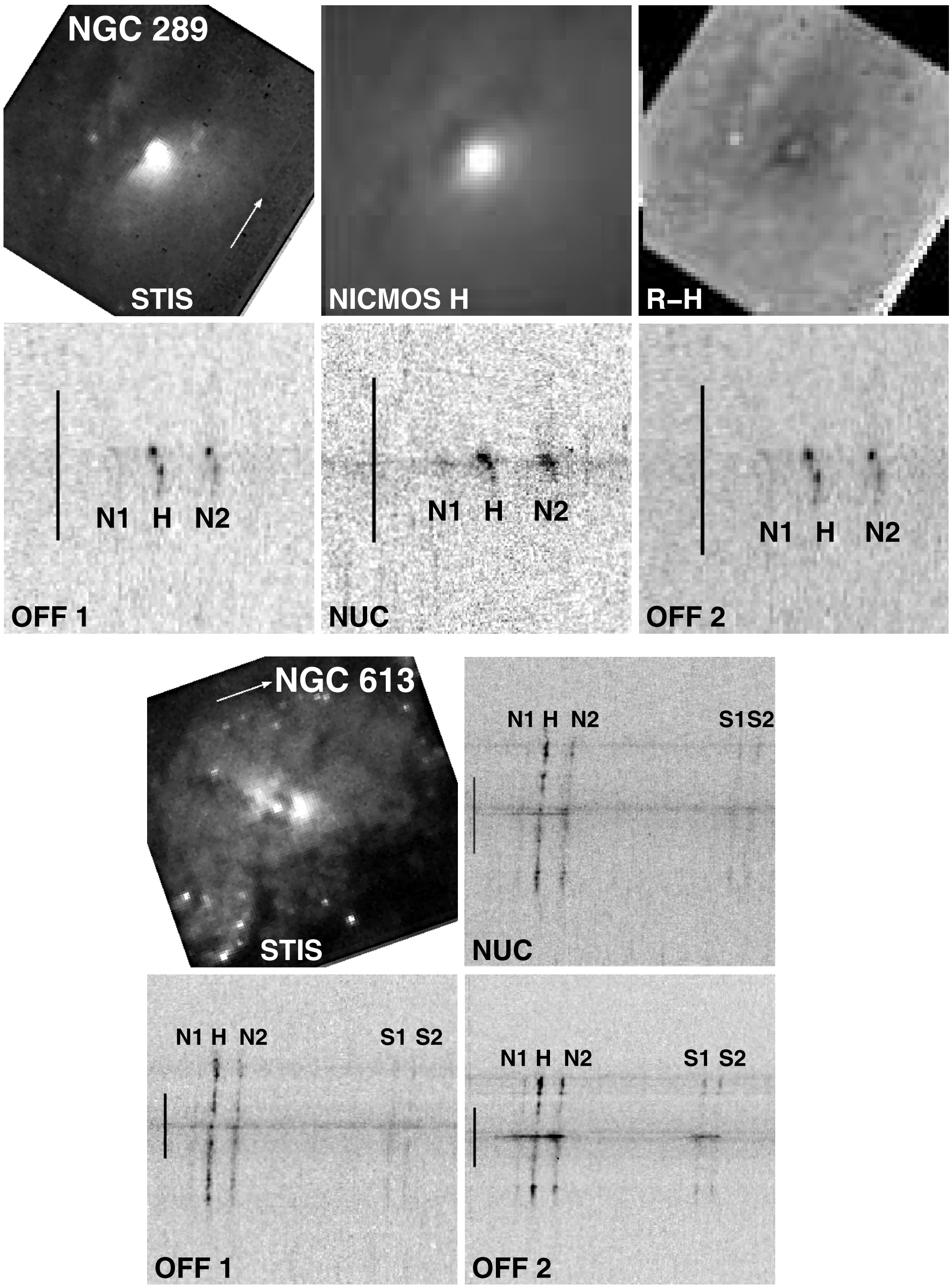

FIG. 1.—Images and spectra for NGC 289 and NGC 613. The scale bars on the spectra indicate a distance of 5″. The images are rotated so that north is up and east is to the left. The white arrow on the STIS image indicates a scale of 1″ and the *y*-direction of the spectroscopic slits. The images have all been unsharp masked to enhance any structures present.

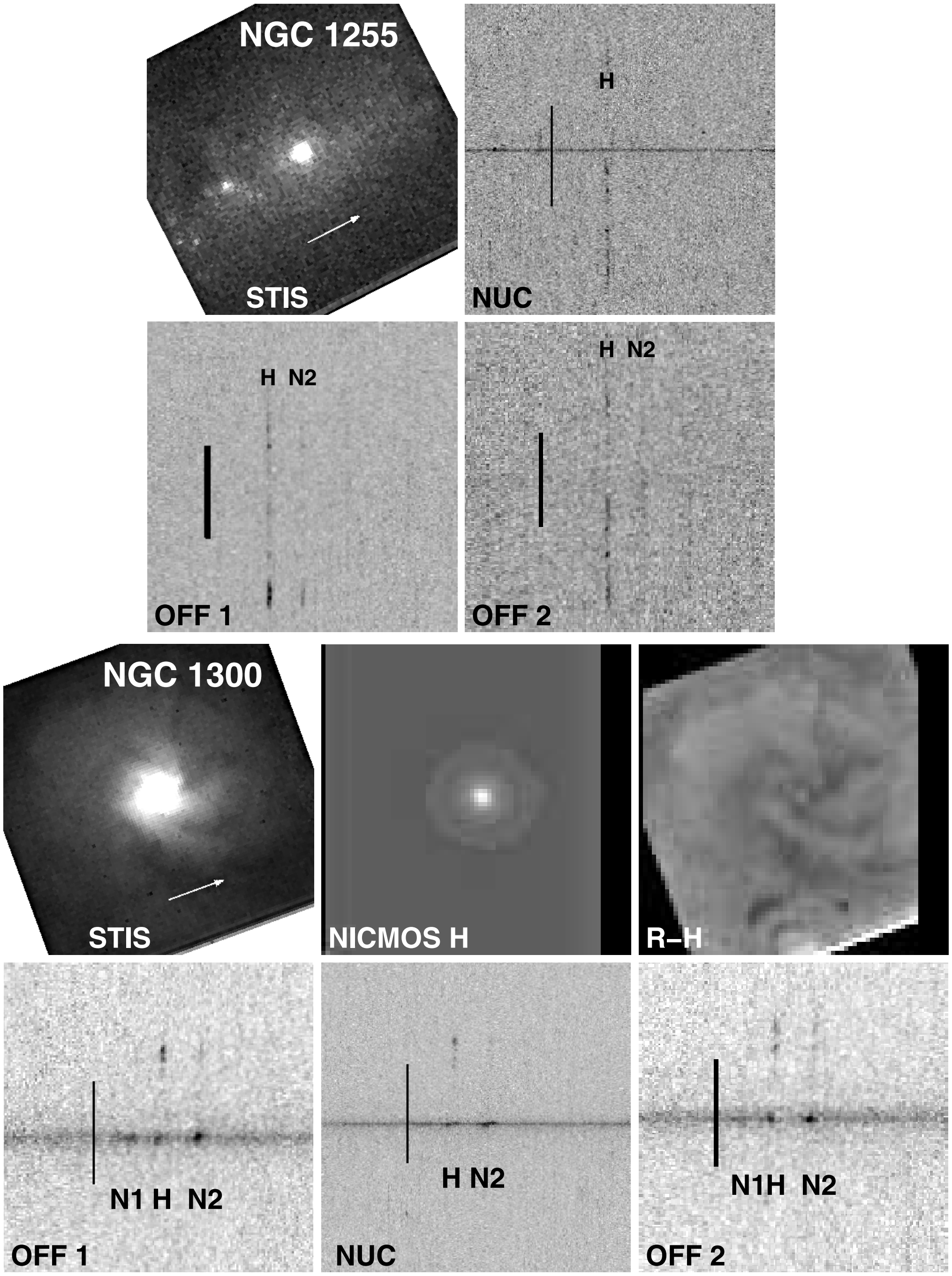

FIG. 2.—Same as Fig. 1, but for NGC 1255 and NGC 1300

located at distances between 6.0 and 24.1 Mpc. These distances correspond to image scales of 29 and 117 pc arcsec^{-1}, respectively.

Those spectra that show clear emission are shown in Figures 1–18. The black bars indicate a scale of 5″. Also shown are the acquisition images that accompany the spectra. All the STIS acquisition images (including those for galaxies without good spectra) are presented in Paper IV. Where possible, archival NICMOS *H*-band images and the resultant *R*−*H* color maps are also shown. Figure 19 shows STIS, NICMOS, and resultant color map images for galaxies where spectra are unavailable. The STIS, NICMOS, and color map images are all rotated so that north is up and east is to the left. All of the images have been unsharp masked to enhance any structures present. The white arrows on the figures indicate both a scale of 1″ and the *y*-direction (along the slit) of the spectroscopic slits.

2.1. *The STIS Spectra*

The spectra of the galaxy centers covered five emission lines [N II] (6549.9 Å), Hα (6564.6 Å), [N II] (6585.3 Å), and [S II] (6718.3 and 6732.7 Å). These spectra were used to map the velocity field of the nuclear gas disk so that the central mass concentration could be determined. Our strategy is described more fully in Paper I. For each galaxy three slits were placed, one on the brightest central source (presumed

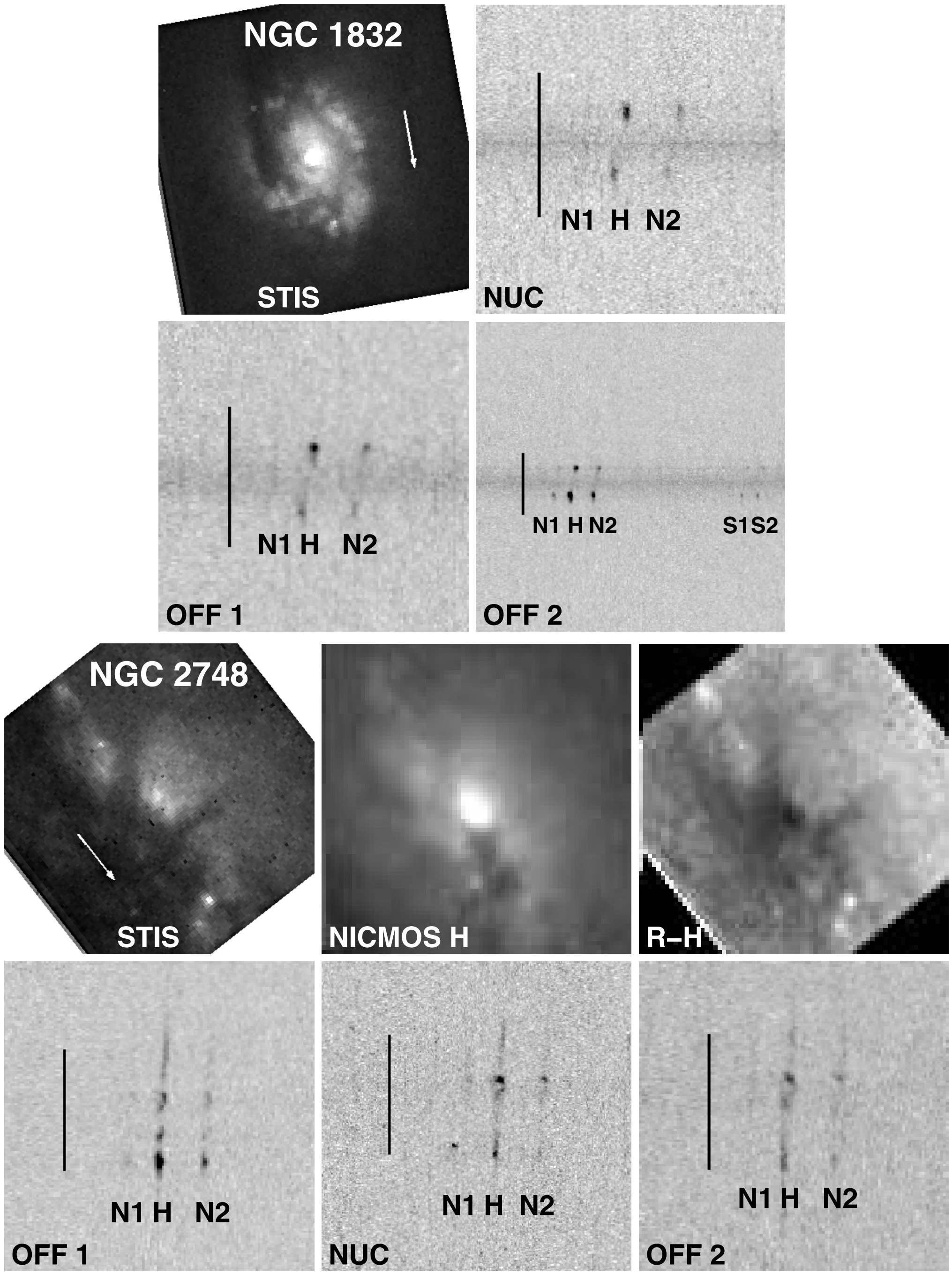

Fig. 3.—Same as Fig. 1, but for NGC 1832 and NGC 2748

to be the nucleus, unless obscured by dust) with two other, parallel slits 0''.2 either side. In all cases the slit widths of the off-nucleus (OFF) slits are 0''.2, although the on-nucleus (NUC) slits are either 0''.1 or 0''.2 in size. For all OFF slits we performed on-chip 2×2 binning, while the NUC slits are either 2×2 binned or unbinned. See Table 1 for a complete description of the slit width and on-chip binning strategy used for each galaxy. In Paper III these spectra will be used to constrain the age of the stellar populations at the centers of the galaxies.

The scale bars shown on the spectra indicate a scale of 5''. Individual emission lines are identified using a key, such that

$$\mathrm{N1} = [\mathrm{N\,II}]\ (6549.9\ \text{Å})\ ,$$
$$\mathrm{H} = \mathrm{H}\alpha\ (6564.6\ \text{Å})\ ,$$
$$\mathrm{N2} = [\mathrm{N\,II}]\ (6585.3\ \text{Å})\ ,$$
$$\mathrm{S1} = [\mathrm{S\,II}]\ (6718.3\ \text{Å})\ ,$$
$$\mathrm{S2} = [\mathrm{S\,II}]\ (6732.7\ \text{Å})\ ,$$

where the wavelengths are for a vacuum. All the galaxies in our sample have significant Hα emission on the large scale;

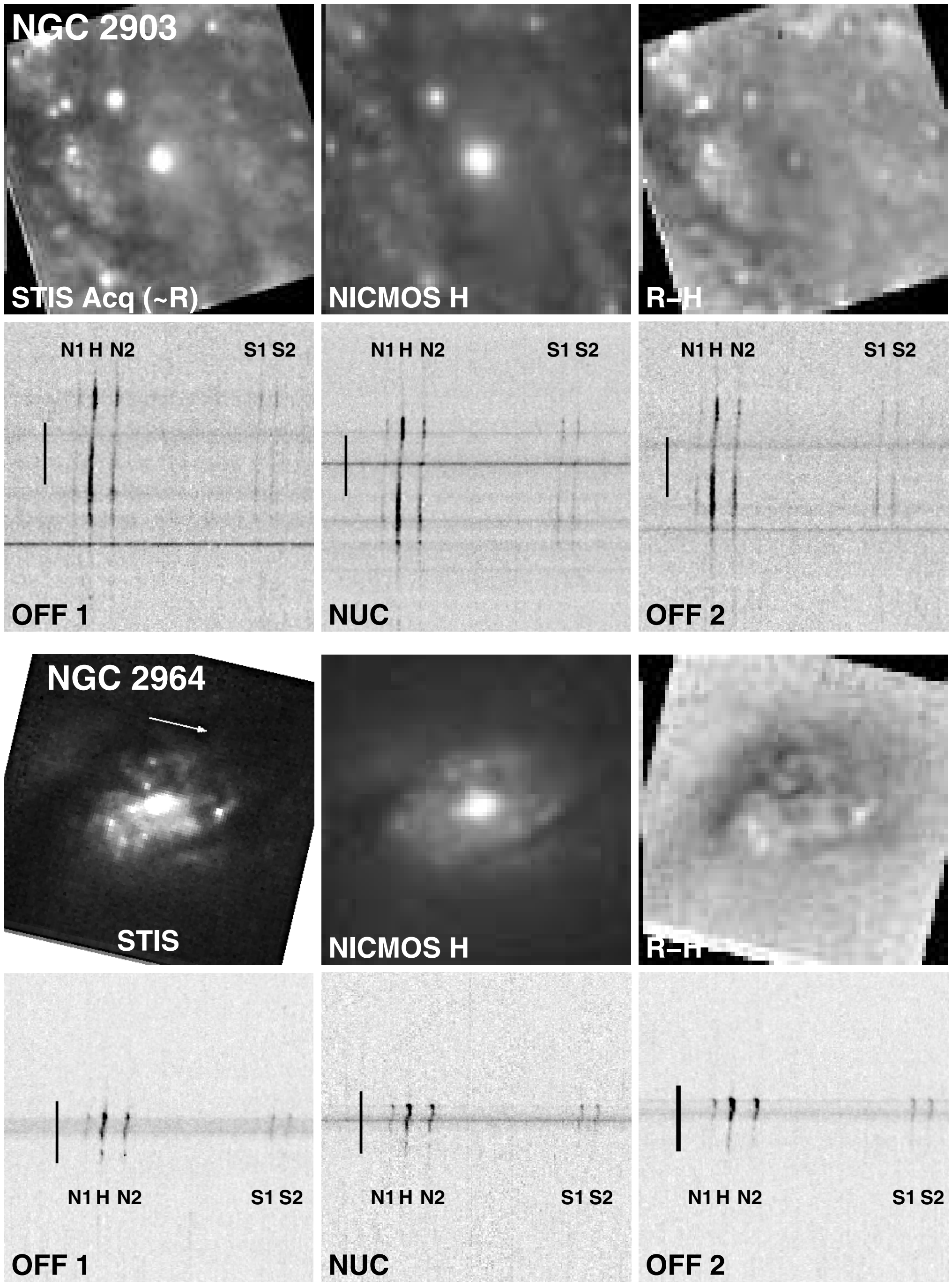

Fig. 4.—Same as Fig. 1, but for NGC 2903 and NGC 2964

however, many show only patchy emission on the scales of these spectra. Significant amounts of obscuring dust are present at the centers of many of these galaxies, particularly near the nuclei. With hindsight, many of these nuclei would be better observed with high-resolution infrared spectroscopy, although this was not obvious before the observations were performed.

Although they all show rather patchy emission, there are significant differences between the spectra. Some spectra, such as for NGC 289, have emission lines but practically no continua. Most spectra do not have obvious [S II] emission, the exceptions being, e.g., NGC 3310 and NGC 4212. Obvious motions, probably rotation of the nuclear gas disks, are seen in the spectra for, e.g., NGC 4536 and NGC 1832, while complicated motions are apparent in the spectra of NGC 5005 and NGC 6951. In several cases, such as for NGC 1832, there is a lack of emission at the center of the galaxy, probably due to dust obscuration.

2.2. *The STIS Acquisition Images*

During each observation of a galaxy, two acquisition images were taken to acquire the nucleus, and three long-slit apertures were placed to determine the nuclear gas disk kinematics.

The STIS images were originally taken to acquire the nucleus of each galaxy so that spectroscopic apertures could

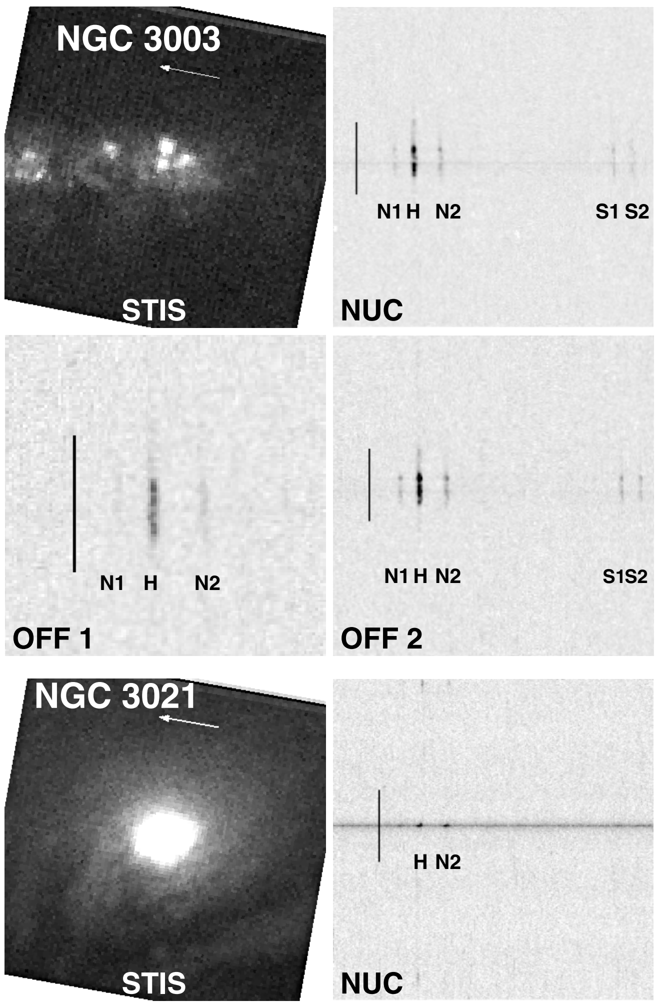

FIG. 5.—Same as Fig. 1, but for NGC 3003 and NGC 3021

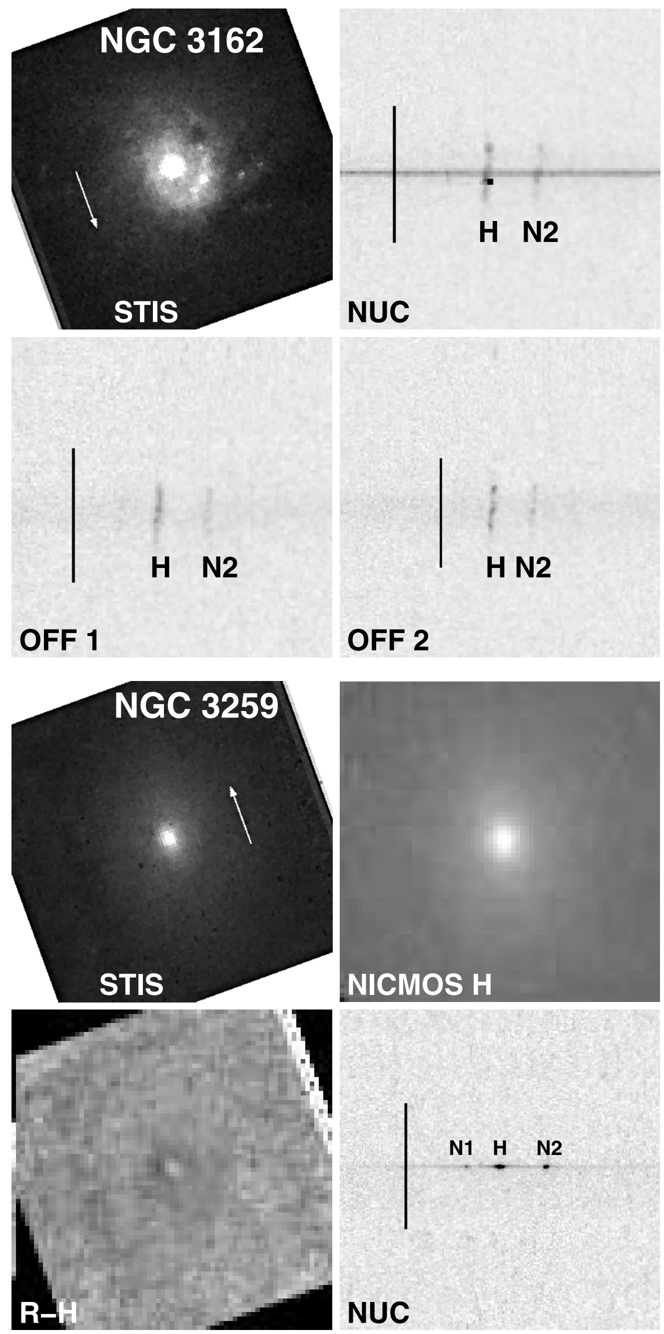

FIG. 6.—Same as Fig. 1, but for NGC 3162 and NGC 3259

be accurately placed. These "acquisition images" were taken using the F28X50LP long-pass filter. They are optical (central wavelength 7230 Å) and are roughly equivalent to *R* band. Two images were taken per visit. The first was based on previous estimates of the nucleus location, and 7×7 boxcar averaging was then used to find the peak intensity, which was assumed to be the location of the nucleus. In the case of galaxies such as NGC 5713 (Fig. 16), the first estimate of the galaxy nucleus was significantly in error such that *HST* was unable to image the nucleus.

The pixel size is $0''.05$ pixel^{-1}, and the field of view is $5'' \times 5''$. Integration times of each image vary between 20 and 60 s. The images were reduced by the flight software, which involves the subtraction of a single bias number and the removal of hot pixels. Details are given in chapter 8 of the STIS Instrument Handbook. Although their original purpose was to locate the nucleus, these images also form a rich data set in their own right.

2.3. *The NICMOS Archival Images*

We searched the *HST* archive for NICMOS observations to complement the STIS images in our sample. We found NIC2 F160W images (similar to a ground-based *H* broadband filter) for 23 galaxies. Many of the images have been observed as part of a snapshot program by members of our team and are presented in Carollo et al. (2002).

The pixel size of the images is $0''.076$ pixel^{-1}, which produces a field of view of $19''.2 \times 19''.2$. The images were taken as part of a number of programs, with integration times of between 384 and 640 s. The images were reduced using NicRed (McLeod 1997). The main steps in the data reduction involved subtraction of the first readout, dark-current subtraction on a readout-by-readout basis, correction for linearity and cosmic-ray rejection (using FULLFIT), and flat-fielding. In-orbit darks with sample sequences and exposure times corresponding to those of the observations were obtained from other programs close in time. Usually between 10 and 20 darks were averaged together (after the

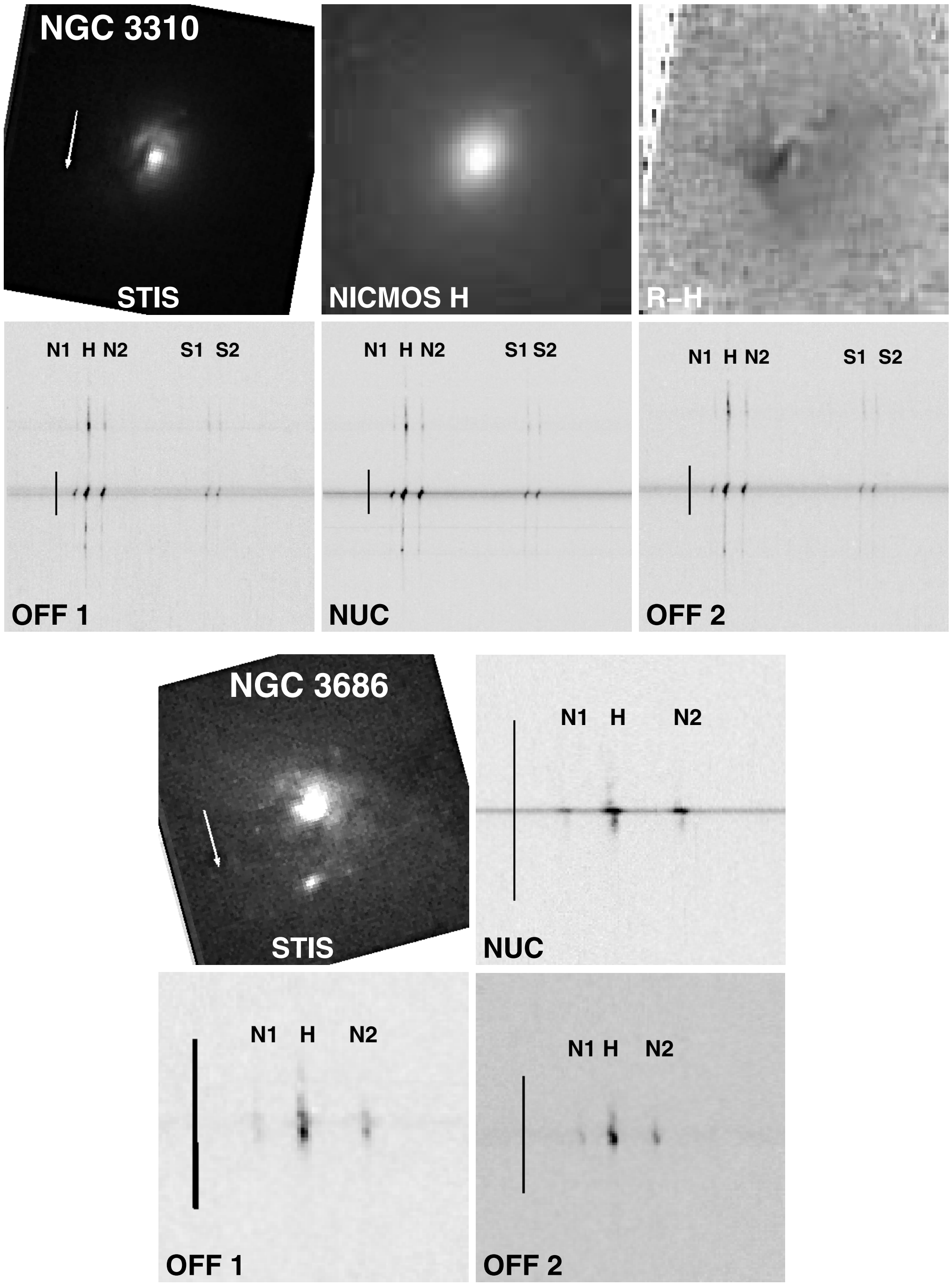

Fig. 7.—Same as Fig. 1, but for NGC 3310 and NGC 3686

subtraction of the first readout) for a given sample sequence. When more than one exposure for a given galaxy was taken, the images were registered to a common position using fractional pixel offsets and were combined to produce the final images. The flux calibration of the NICMOS images was performed using conversion factors (from ADU s^{-1} to Jy) based on measurements of the standard star P330-E taken during the Servicing Mission Observatory Verification program (M. J. Rieke 1999, private communication).

2.4. *Morphological Features in the Images*

The spatial resolution of the images (as measured from point sources) is approximately $0\farcs07$ and $0\farcs14$ for the STIS acquisition and NIC2 F160W images, respectively. To create the color maps, the STIS and NICMOS images were rotated so that north was up and east to the left for both images. The STIS images were then magnified from a pixel size of $0\farcs05$ pixel^{-1} to the NICMOS pixel size of $0\farcs076$ pixel^{-1}. After locating the center of the nucleus in each galaxy, we divided each of the STIS images by the corresponding NICMOS image. While the mismatch in point-spread functions means that the color maps cannot be trusted at their centers, the effect is not significant for the general interpretation of their nuclear morphology as discussed in this paper. In the color maps darker pixels are redder and so suggest the presence of dust. Although a NICMOS image was

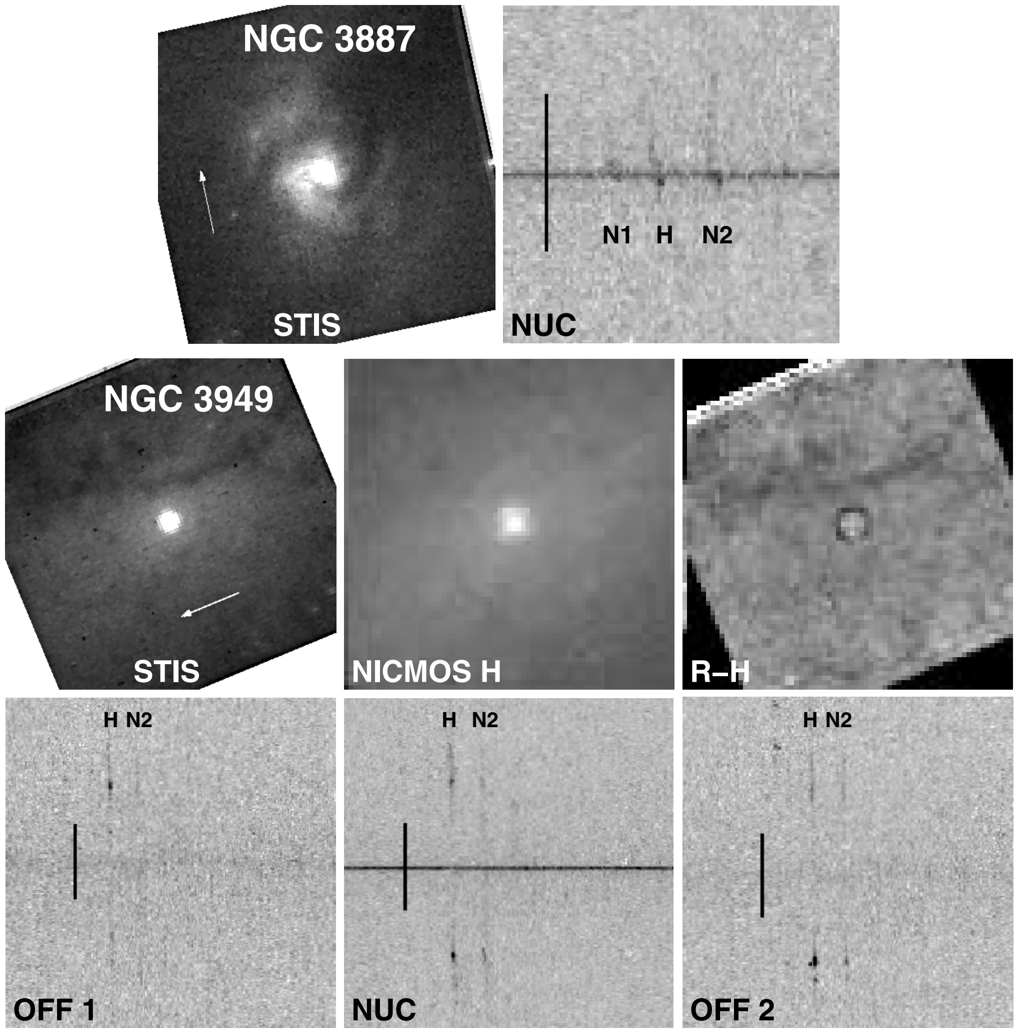

Fig. 8.—Same as Fig. 1, but for NGC 3887 and NGC 3949. An Airy ring can be seen in the NICMOS image and color map for NGC 3949.

available for NGC 5577, there are no clear nuclear or point-like features in the images for accurate alignment, so color maps were not produced.

The high spatial resolution of *HST* ($\sim0''.1$) allows us to resolve 10 pc features at a typical distance of 20 Mpc. Not surprisingly, in recent years *HST* has played a pivotal role in producing detailed images of galactic central regions. Large samples of spiral galaxies have been observed using the *HST* Wide Field Planetary Camera 2 (Carollo, Stiavelli, & Mack 1998; Carollo et al. 1997; Böker et al. 2002) and *HST*/NICMOS (Carollo et al. 2001, 2002; Seigar et al. 2002). Such studies have revealed that galactic centers can contain remarkably complex structures. Morphological features such as bars, rings, and stellar clusters are often resolved at these scales. One particularly interesting feature is the presence of nuclear spiral arms on scales of only a few hundred parsecs, so-called nuclear (or mini-) spirals (e.g., Ford et al. 1994; Elmegreen et al. 1998; Martini & Pogge 1999; Regan & Mulchaey 1999; Pérez et al. 2000; Laine et al. 2001). These nuclear spirals often look remarkably like their large-scale counterparts, although they tend to be primarily dust, rather than stellar, structures. Martini & Pogge (1999) proposed that nuclear spirals might be the mechanism by which gas is transported to galaxy centers. Maciejewski et al. (2002) have recently modeled gas inflow and find that at high sound speed, gas can flow to the center through a "nuclear in-spiraling shock."

A wide range of morphologies, from organized structures such as nuclear spirals to smooth, almost featureless distributions, are apparent in the images in this paper. Many of the galaxies have considerable amounts of dust near the nucleus, and it would be desirable to see these galaxies, at similar resolutions, in the infrared. The NICMOS *H*-band images allow us to investigate these structures more fully. Despite the similarities in the large-scale morphological type of these galaxies, the small-scale structures vary significantly from galaxy to galaxy. For example, both NGC 3259 and NGC 4303 are classified as SAB(rs)bc (NASA/IPAC Extragalactic Database [NED]), yet the color map of the former appears smooth and featureless, while for the latter, a clear nuclear spiral is present.

Extensive work has been done by Pogge & Martini (2002) and Martini et al. (2003) to investigate nuclear spirals in statistically significant samples. Martini et al. (2003) found that nuclear spirals were the most common morphological feature in galaxy centers and have recently introduced a new classification scheme for creating a nuclear spiral taxonomy. In particular, they define five classes: " grand design nuclear

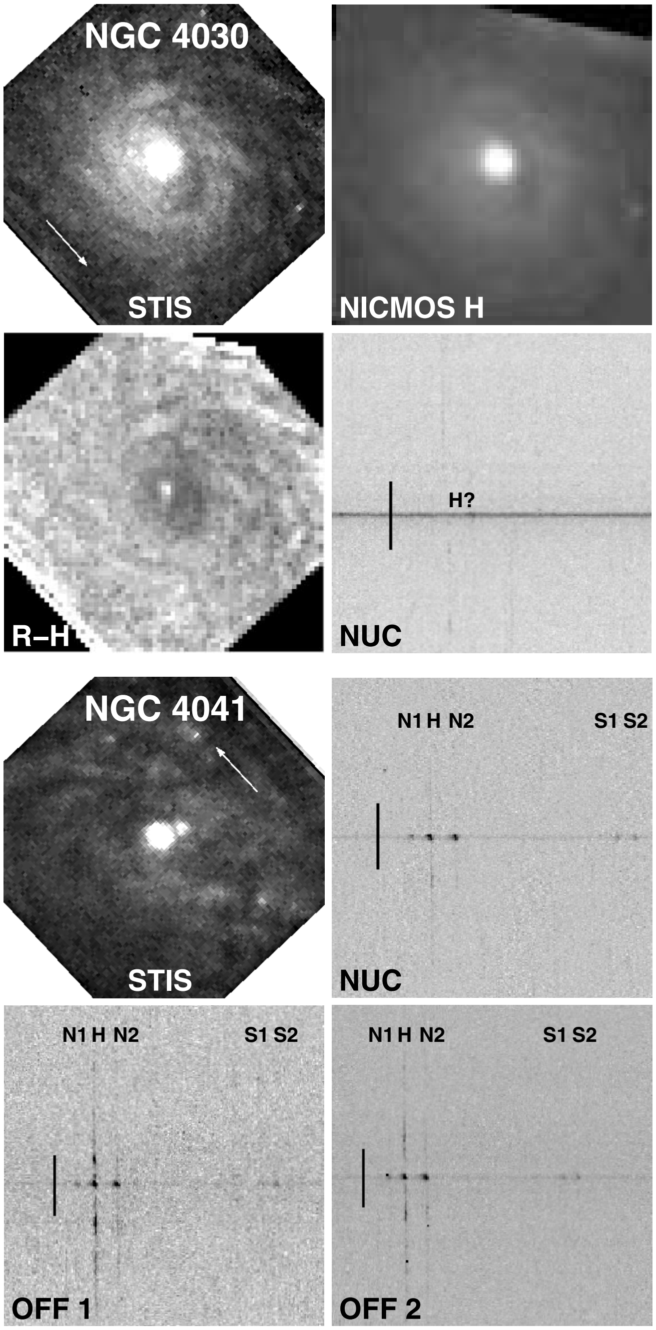

Fig. 9.—Same as Fig. 1, but for NGC 4030 and NGC 4041

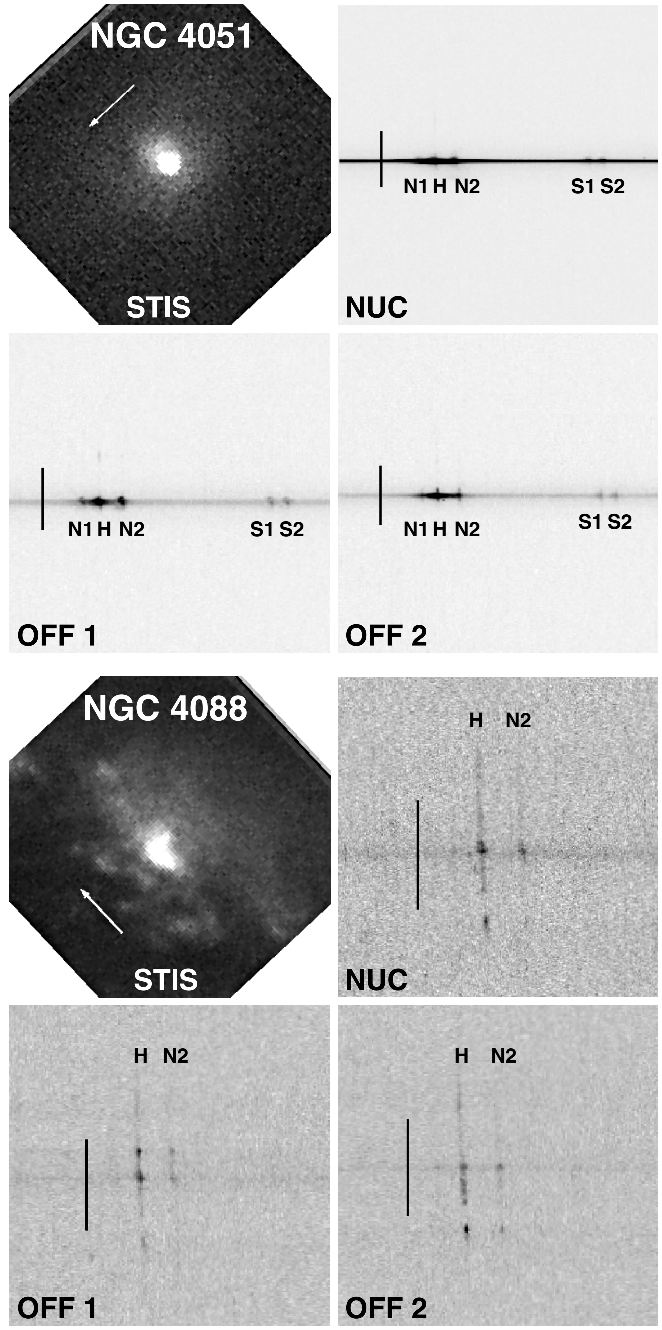

Fig. 10.—Same as Fig. 1, but for NGC 4051 and NGC 4088

spirals'' (GD), ''tightly wound nuclear spirals'' (TW), ''loosely wound nuclear spirals'' (LW), ''chaotic nuclear spirals'' (CS), ''chaotic circumnuclear dust'' (C), and galaxies for which there is ''no structure'' (N). Martini et al. (2003) classify eight of the galaxies from our sample using this system: NGC 1300 (GD), NGC 2903 (C), NGC 4030 (TW), NGC 4303 (GD), NGC 5005 (C), NGC 5054 (LW), NGC 6384 (C), and NGC 6951 (LW). NGC 4258 is also in their sample, but they find that the inclination of the galaxy is too high to use their classification system.

The images in this paper are typically only $5'' \times 5''$, and so fitting them to the Martini et al. (2003) classification is not simple, since some features may only be obvious on larger scales. However, in § 3 we classify those galaxies for which we have produced color maps. One slight change is our use of the ''chaotic circumstellar dust'' classification, which is defined by Martini et al. (2003) for all galaxies where there is dust but no obvious spiral structure. Using this scheme would mean that those galaxies that have discernible dust lanes near their centers would have the same classification as those with truly chaotic dust features. To distinguish between these cases we introduce here a ''dust lanes'' (DL) category to indicate galaxies with organized dust features that do not appear to be part of a spiral structure. It must be noted, however, that this may only be a temporary ''holding'' category and that larger scale images may reveal that such galaxies need to be recategorized as nuclear spirals.

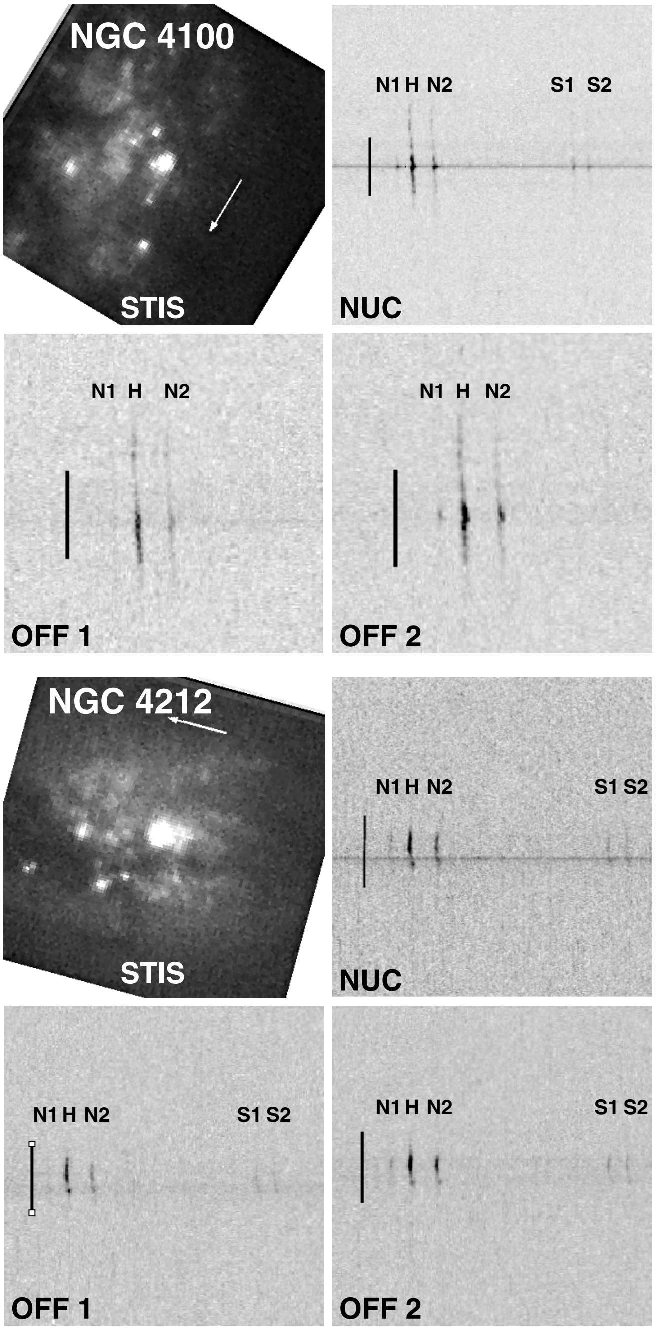

FIG. 11.—Same as Fig. 1, but for NGC 4100 and NGC 4212

3. COMMENTS ON SPECTRA AND IMAGES FOR INDIVIDUAL GALAXIES

The morphological classification as determined by us is indicated in parentheses next to the galaxy name, with our "chaotic circumnuclear dust" (C) category now not including those galaxies with obvious dust lanes (DL). Where the classification has already been made by Martini et al. (2003), we indicate this with "-mp."

3.1. *NGC 157: Spectacular Nuclear Dust Lane* (*DL*)

Figure 19 (*top*). Images: NGC 157 is a spectacular example of why infrared observations are sometimes vital for studying the centers of spiral galaxies. In the STIS image the nucleus is completely obscured by a V-shaped dust lane, and yet in the NICMOS image the nucleus appears smooth and unobscured. The presence of the dust lane meant that we were not able to acquire the true nucleus for the spectroscopy. Hence, the spectra quality is classified as "missed" in Table 1.

3.2. *NGC 289* (*C*)

Figure 1 (*top*). Spectra: There is a weak continuum and little extended emission, but the Hα and [N II] emission lines show characteristics of rotation. Images: As noted by Carollo et al. (2002), a dust lane runs from the northwest to the southeast, close to the nucleus.

3.3. *NGC 613*

Figure 1 (*bottom*). Spectra: The continuum is generally weak; there is large-scale extended patchy emission with broad emission lines in OFF 2 and NUC spectra. In the NUC spectrum the broad feature appears to be located $\sim 0\farcs4$ from the principal continuum. Image: Hummel & Jorsater (1992) found from Very Large Array observations that NGC 613 has a complex nuclear geometry when observed in radio emission. They found a central elongated region of three distinct components $\sim$300 pc in length (assuming a distance of 19 Mpc to the galaxy). They also found an arc feature $\sim$350 pc from the nucleus.

3.4. *NGC 1255*

Figure 2 (*top*). Spectra: Emission is patchy and faint, with very little emission near the center of the galaxy. Continuum is obvious only in the NUC spectrum.

3.5. *NGC 1300* (*GD-mp*)

Figure 2 (*bottom*). Spectra: There is some continuum and a broad feature on NUC spectrum. Generally, emission lines are faint. Images: Color map shows spiral structure down to the resolution of nucleus.

3.6. *NGC 1832*

Figure 3 (*top*). Spectra: There is practically no continuum. Rotation is indicated by two blobs present for each line, but there is a lack of emission in between these features.

3.7. *NGC 2748* (*C*)

Figure 3 (*bottom*). Spectra: Very patchy emission. There is some large-scale rotation, but it is not obvious for central regions. Images: STIS image shows spider-like dust lanes, which are not seen in the NICMOS image.

3.8. *NGC 2903* (*C*) (*C-mp*)

Figure 4 (*top*). Spectra: They show strong emission, although the continuum is strong only in the NUC spectrum. Rotation is clear on large scale. There is secondary continuum in the OFF 1 spectrum. Images: A hotspot galaxy; Alonso-Herrero, Ryder, & Knapen (2001) find a circumnuclear star formation ring of diameter 625 pc in their *HST*/NICMOS images. This ring would appear just outside of our images.

3.9. *NGC 2964* (*C*)

Figure 4 (*bottom*). Spectra: Strong emission lines near continuum center, including obvious [S II] emission lines.

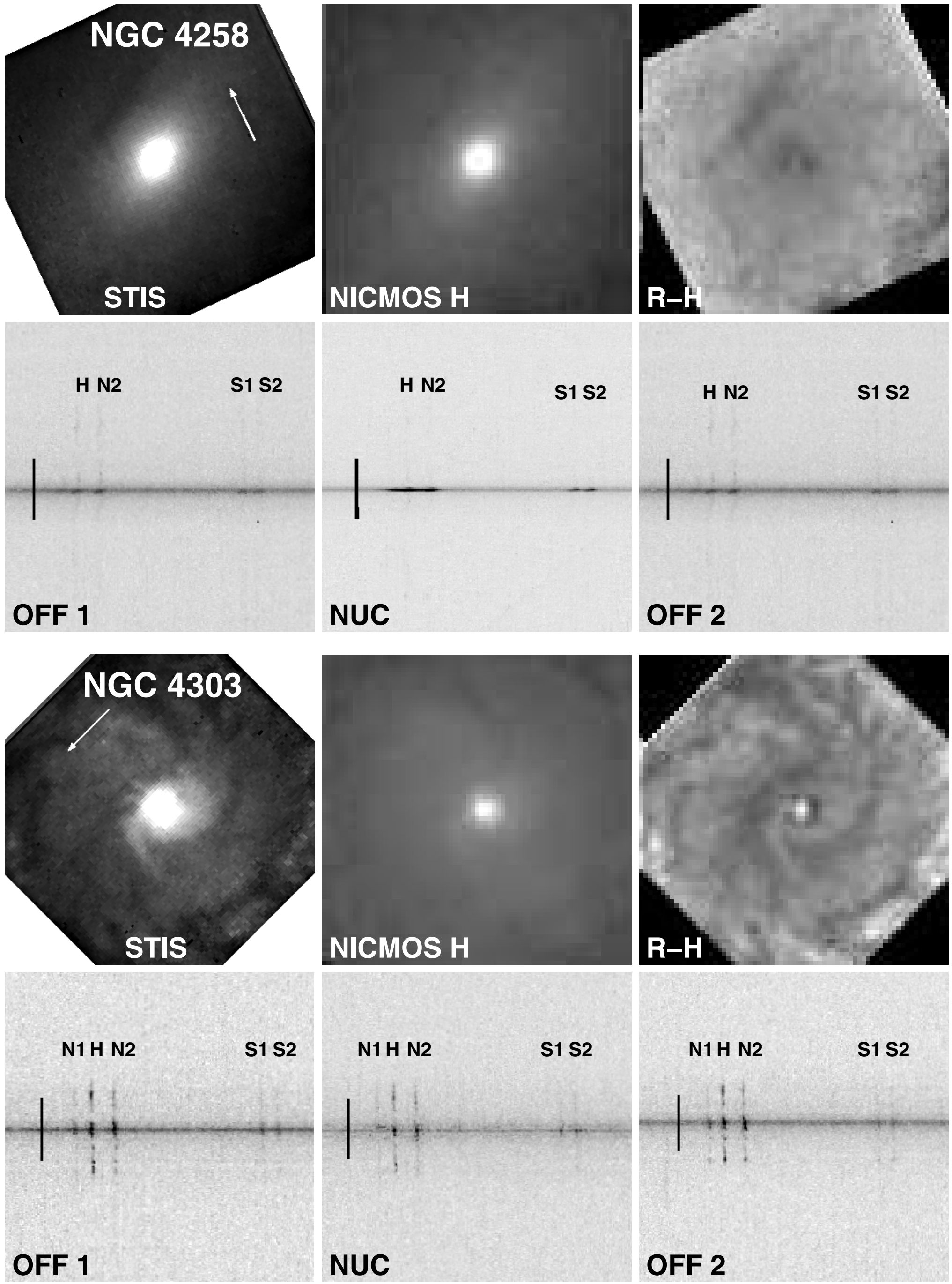

FIG. 12.—Same as Fig. 1, but for NGC 4258 and NGC 4303

Continuum is generally weak. Images: Carollo et al. (2002) find a spiral structure and red dust features down to the nucleus. In these images we see a possible ring or spiral structure obscured by significant amounts of dust, as demonstrated in the color map.

3.10. *NGC 3003*

Figure 5 (*top*). Spectra: Strong emission in Hα and other lines is obvious in the OFF 2 and NUC spectra. There is no obvious signs of rotation. The continuum is weak in each spectrum. Images: Three cluster-like features in the center. The location of the nucleus is not obvious.

3.11. *NGC 3021*

Figure 5 (*bottom*). Spectra: Very little emission in either continuum or emission lines. Some emission features on NUC spectrum.

3.12. *NGC 3162*

Figure 6 (*top*). Spectra: A continuum is present only in the NUC spectrum. Hα and one [N II] line are present in all spectra. There is some evidence of rotation.

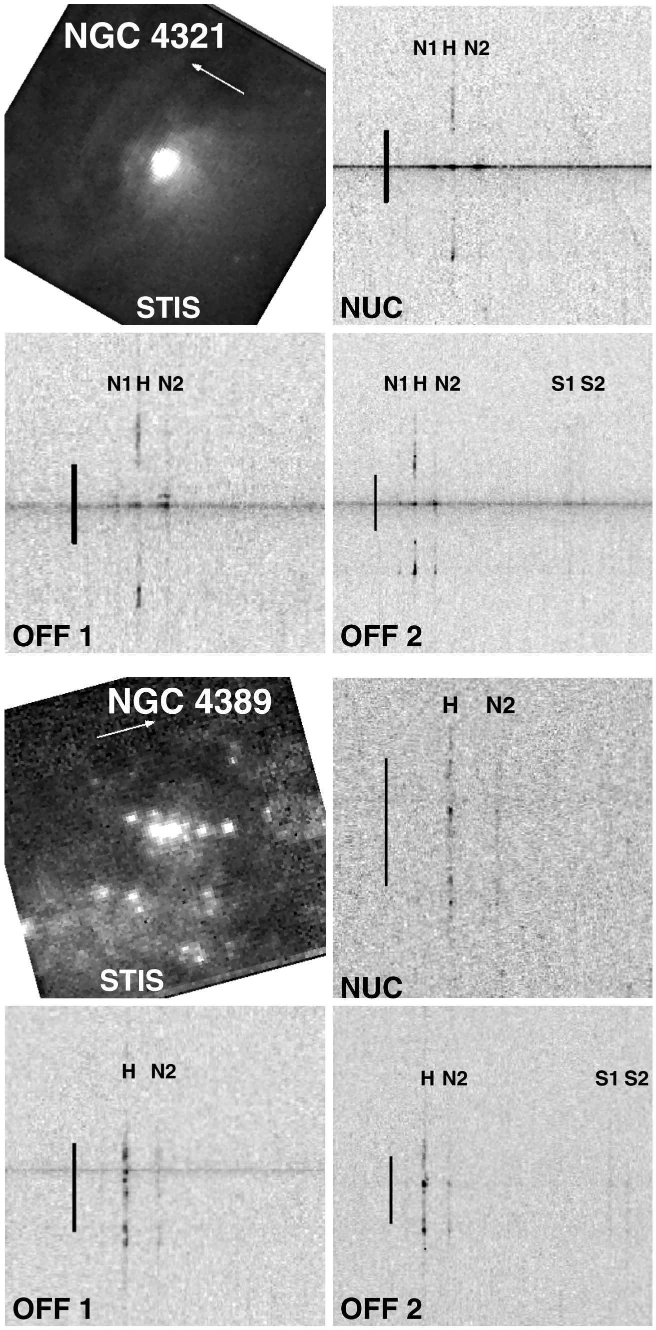

FIG. 13.—Same as Fig. 1, but for NGC 4321 and NGC 4389

3.13. *NGC 3259* (*N*)

Figure 6 (*bottom*). Spectrum: Obvious evidence of emission is present only in the NUC spectrum. Images: Carollo et al. 2002 find "flocculent nuclear blue spiral arms and red (dust) lanes." However, these images appear smooth and almost featureless.

3.14. *NGC 3310: An Inner Circumnuclear Ring?* (*C*)

Figure 7 (*top*). Spectra: The spectra are among the best in the sample, showing clear emission lines and obvious rotation. There is evidence for H II regions. Images: NGC 3310 is a well-known site of circumnuclear star formation and has been studied extensively by many authors (see Elmegreen et al. 2002 for a recent review). The STIS image shows an arc 0″.5 (~40 pc) north of the galactic center. The color map shows this feature to be bluer than the surrounding medium, indicating that the arc may be part of an inner circumnuclear star formation ring. The $R-H$ color map, shown in Figure 7, shows that there are significant amounts of dust present at the center of this galaxy, which would be consistent with a partially obscured ring.

3.15. *NGC 3686*

Figure 7 (*bottom*). Spectra: A continuum is obvious only in the NUC spectrum, which also shows a broad component to the lines.

3.16. *NGC 3887*

Figure 8 (*top*). Spectrum: Hα and [N II] emission is weak and is obvious only in the NUC spectrum.

3.17. *NGC 3949* (*DL*)

Figure 8 (*bottom*). Spectra: Continuum only in the NUC spectrum. Only extended emission lines are present in any of the spectra. Images: Carollo et al. (2002) find a photometrically distinct nucleus, a barlike feature, and a red dust lane 0″.7 north of the nucleus. A bar cannot be seen in these images; however, the thin dust lane is clear in the STIS image and color map.

3.18. *NGC 4030* (*CS*) (*TW-mp*)

Figure 9 (*top*). Spectrum: Only the continuum is obvious in the NUC spectrum. Images: A faint spiral structure can be seen going down to the nucleus but is not obvious in the NICMOS image.

3.19. *NGC 4041*

Figure 9 (*bottom*). Spectra: Hα and [N II] emission lines are present in all of the spectra. This was the first galaxy observed in the program, and the results of the modeling are reported in Paper I. Image: The STIS images show two blobs, one of which should be the nucleus.

3.20. *NGC 4051*

Figure 10 (*top*). Spectra: Strong broad features with little extended emission. Continuum is strong only in the NUC spectrum.

3.21. *NGC 4088*

Figure 10 (*bottom*). Spectra: The continuum is weak in each spectrum, but emission lines are present at the continua centers. Patchy extended emission is present in all of the spectra.

3.22. *NGC 4100*

Figure 11 (*top*). Spectra: A continuum is present only in the NUC spectrum. All lines (i.e., Hα, both [N II], and both [S II]) are present in the NUC spectrum. The velocity field seems complicated. Is the gas disturbed?

3.23. *NGC 4212*

Figure 11 (*bottom*). Spectra: There is only weak continuum on the NUC spectrum. There are banana-shaped emission lines indicating rotation.

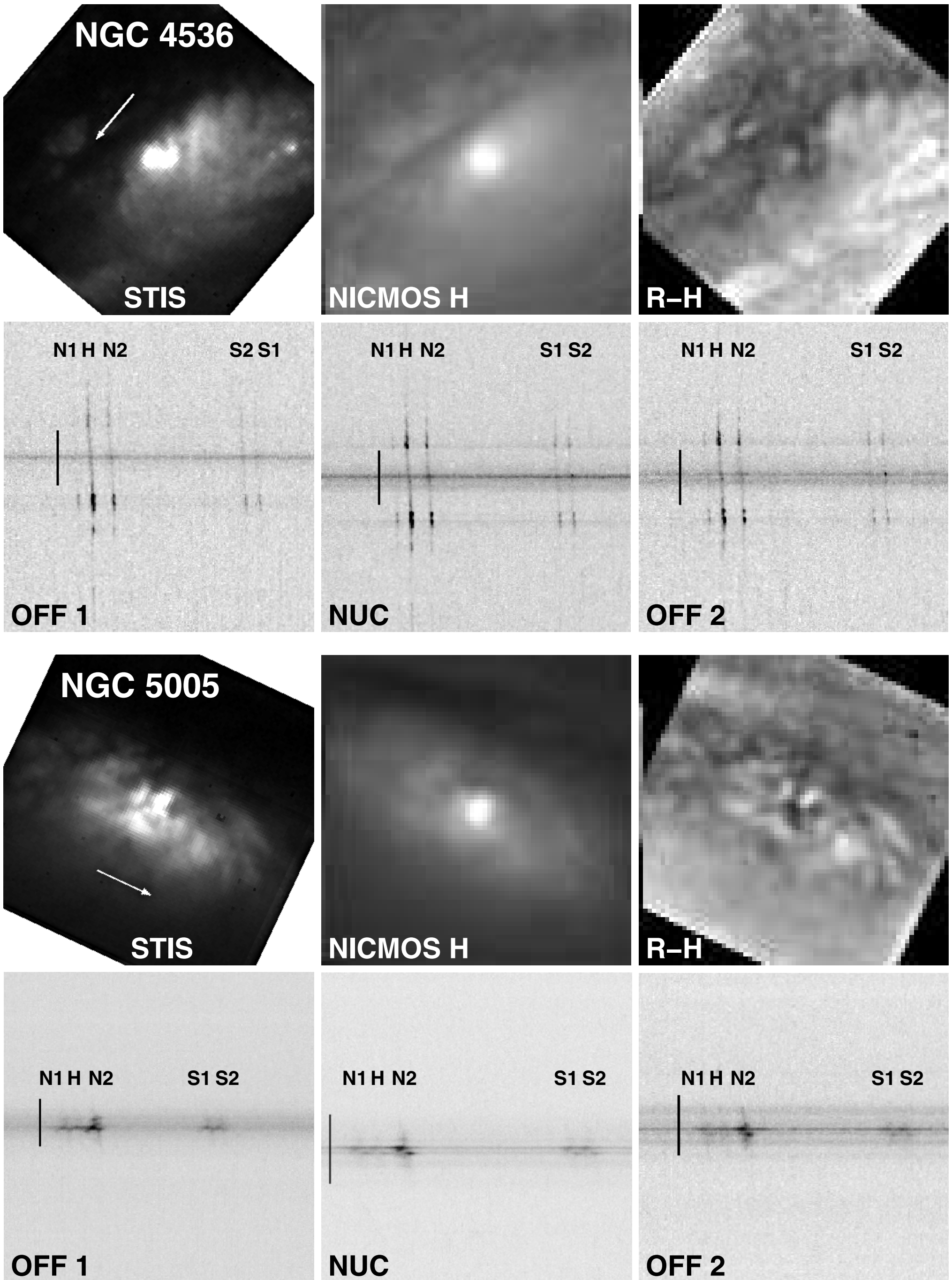

Fig. 14.—Same as Fig. 1, but for NGC 4536 and NGC 5005

3.24. *NGC 4258* (*DL*)

Figure 12 (*top*). Spectra: Broad emission lines on NUC spectrum, with little extended emission. Lines are less broad in OFF spectra, but more extended emission is present. Images: Smooth profile, with dust lane to the northeast of the nucleus.

3.25. *NGC 4303* (*GD*) (*GD-mp*)

Figure 12 (*bottom*). Spectra: Patchy, but emission is present for all lines. Rotation is not obvious. Images: Spiral structure down to nucleus.

3.26. *NGC 4321*

Figure 13 (*top*). Spectra: Some patchy extended emission lines. These lines do not join to the line emission at the continuum center. There is strong continuum on the NUC spectrum.

3.27. *NGC 4389*

Figure 13 (*bottom*). Spectra: Continuum is obvious only in OFF 1 and appears weak. H II regions are indicated in the spectra, agreeing with Alonso-Herrero & Knapen (2001), who find multiple H II sites in the galaxy. The emission lines

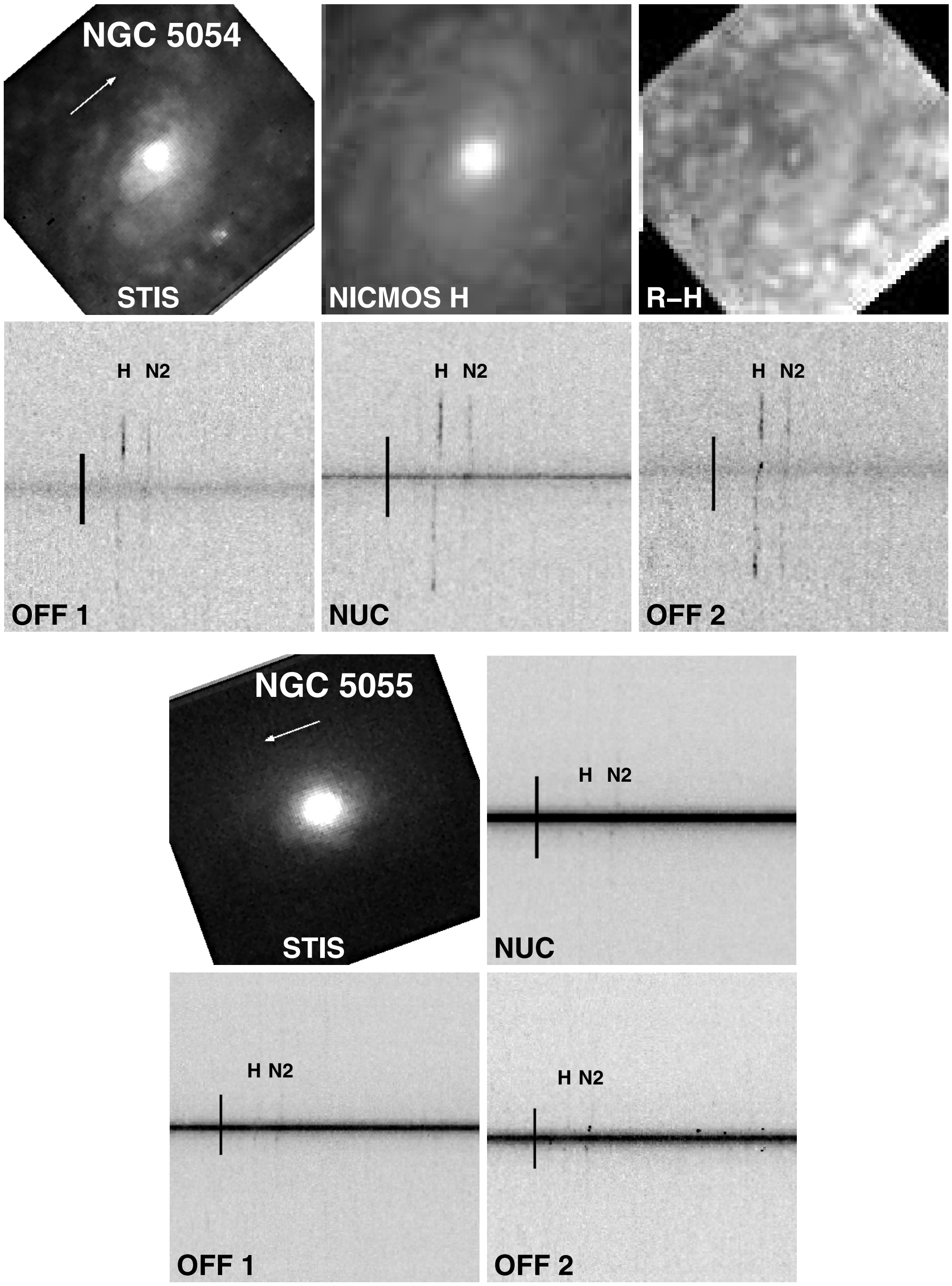

FIG. 15.—Same as Fig. 1, but for NGC 5054 and NGC 5055

appear straight. Image: Location of nucleus is not obvious since it is difficult to distinguish from probable sites of star formation.

3.28. *NGC 4527* (*C*)

Figure 19 (*second from top*). Images: Irregular structure in both the STIS and NICMOS images because of obscuring dust.

3.29. *NGC 4536* (*C*)

Figure 14 (*top*). Spectra: Strong continuum and emission lines and clear evidence of rotation. Images: Obscuring dust to the northeast of the nucleus in both STIS and NICMOS images.

3.30. *NGC 5005* (*C*) (*C-mp*)

Figure 14 (*bottom*). Spectra: Complicated emission-line structure. The continua are generally weak. Emission does not extend to large distances. Images: Complicated dust morphology.

3.31. *NGC 5054* (*CS*) (*LW-mp*)

Figure 15 (*top*). Spectra: A continuum obvious only in the NUC spectrum. There are patchy extended emission lines.

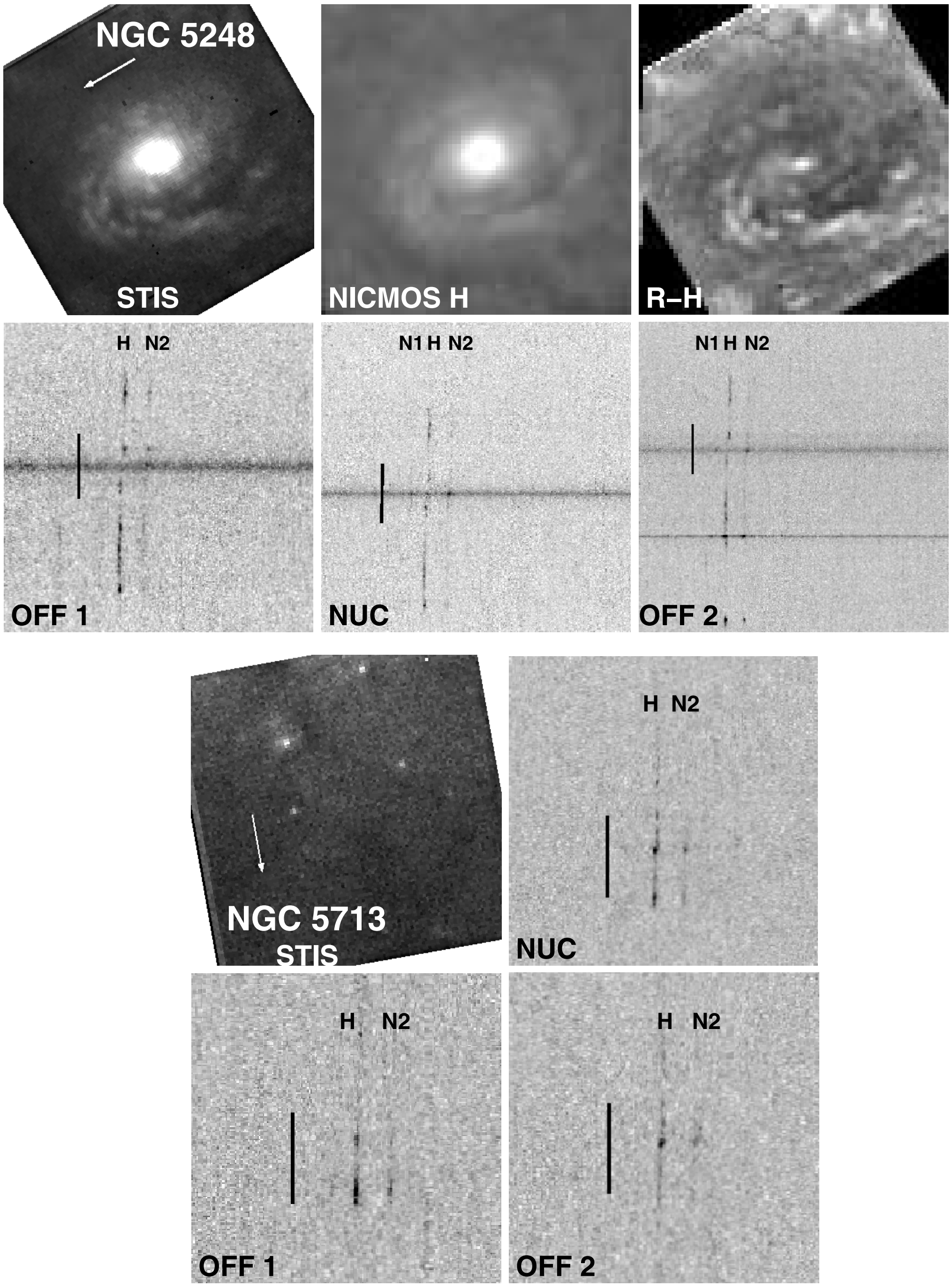

Fig. 16.—Same as Fig. 1, but for NGC 5248 and NGC 5713. The acquisition image for NGC 5713 did not include the center of the galaxy, but since there are emission lines in the spectra, the data are included here.

Hα in OFF 2 shows the best evidence for rotation. Images: Star-forming regions to the south of nucleus?

3.32. *NGC 5055*

Figure 15 (*bottom*). Spectra: Very strong continuum, which almost swamps the emission lines. However, these faint emission lines show clear rotation.

3.33. *NGC 5248: A Stellar Nuclear Spiral Arm* (*GD?*)

Figure 16 (*top*). Spectra: The spectra show patchy Hα and [N II] emission. Continua are weak. A secondary continuum is present in OFF 2. Classified in NED as either H II or Seyfert, but our spectra show no evidence for broad lines. Images: One of the clearest nuclear spirals in the sample. Laine et al. (2001) have previously investigated the two-dimensional velocity field of NGC 5248. They conclude that the pattern speed of the nuclear spiral is the same as for the large-scale spiral structure, implying that they are coupled. In the images shown here, only one spiral arm is clearly present. The $R-H$ color map shows it to be a blue feature, probably a site of star formation.

3.34. *NGC 5713*

Figure 16 (*bottom*). Spectra: No continuum, but faint, patchy lines. There is no obvious rotation. Image: The

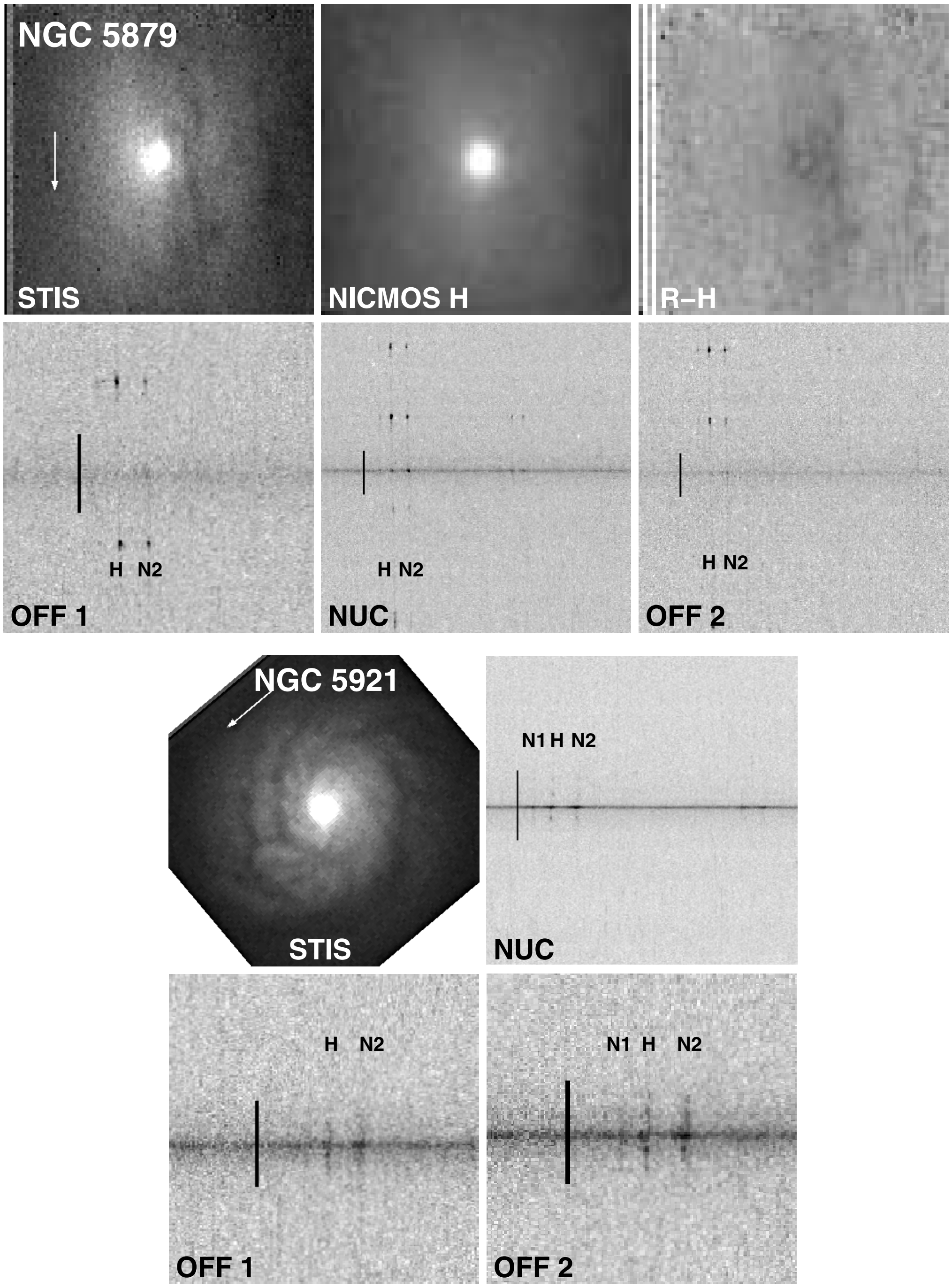

FIG. 17.—Same as Fig. 1, but for NGC 5879 and NGC 5921

galaxy nucleus was not acquired, but since the spectra show emission, they are included here.

3.35. *NGC 5879* (*DL*)

Figure 17 (*top*). Spectra: Faint continua and lines. Also H II regions? Images: There is a north-south dust lane in the STIS image that is not present in the NICMOS image.

3.36. *NGC 5921*

Figure 17 (*bottom*). Spectra: Emission lines and continua are very faint.

3.37. *NGC 6384* (*DL*) (*C-mp*)

Figure 19 (*third from top*). Images: Both the STIS and the NICMOS images appear smooth and almost featureless.

3.38. *NGC 6951: Intricate Dust Structure* (*GD*) (*LW-mp*)

Figure 18 (*top*). Spectra: The spectra show strong and complex emission-line features. Some broad features are present in the spectra. The continua appear faint. Images: The color map of NGC 6951 displays intricate dust lanes, forming a weblike appearance. These features have been seen before by Pérez et al. (2000) and are emphasized by these *HST* images.

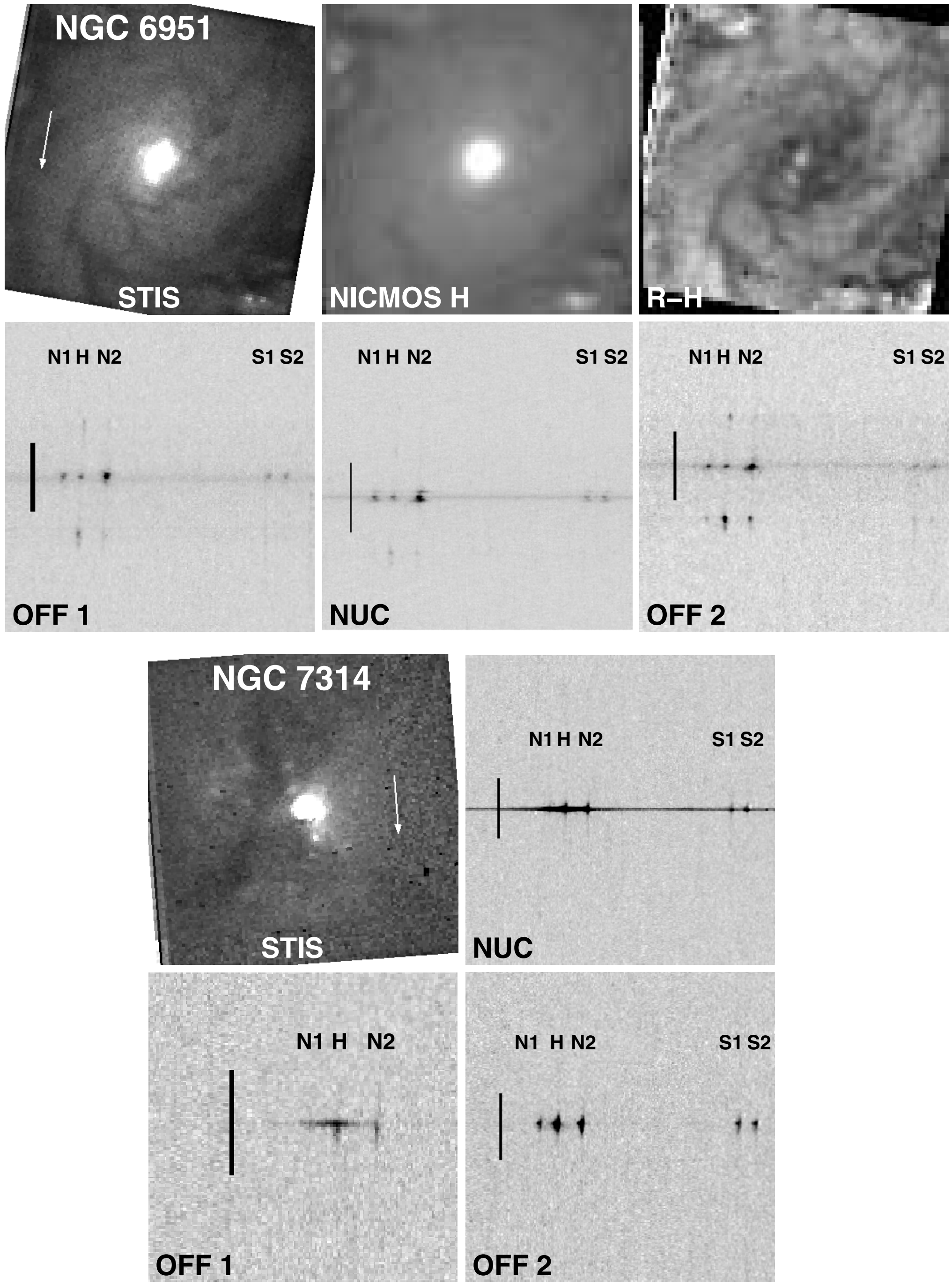

Fig. 18.—Same as Fig. 1, but for NGC 6951 and NGC 7314

3.39. *NGC 7314*

Figure 18 (*bottom*). Spectra: Strong broad lines with a continuum present only in NUC spectrum. Consistent with classification as a Seyfert 1.9.

3.40. *NGC 7331* (*DL*)

Figure 19 (*bottom*). Images: Smooth in both NICMOS and STIS images, with a dust lane along the western edge of the color map.

4. SUMMARY

In this paper we use archival NICMOS images to produce color maps to further highlight dust features. The color maps emphasize that many of the galaxies have prominent dust features at their centers but that morphology can vary significantly between different galaxies. As has been found by other authors (e.g., Carollo et al. 1998; Martini & Pogge 1999; Laine et al. 2001), some galaxies have nuclear spirals at their centers.

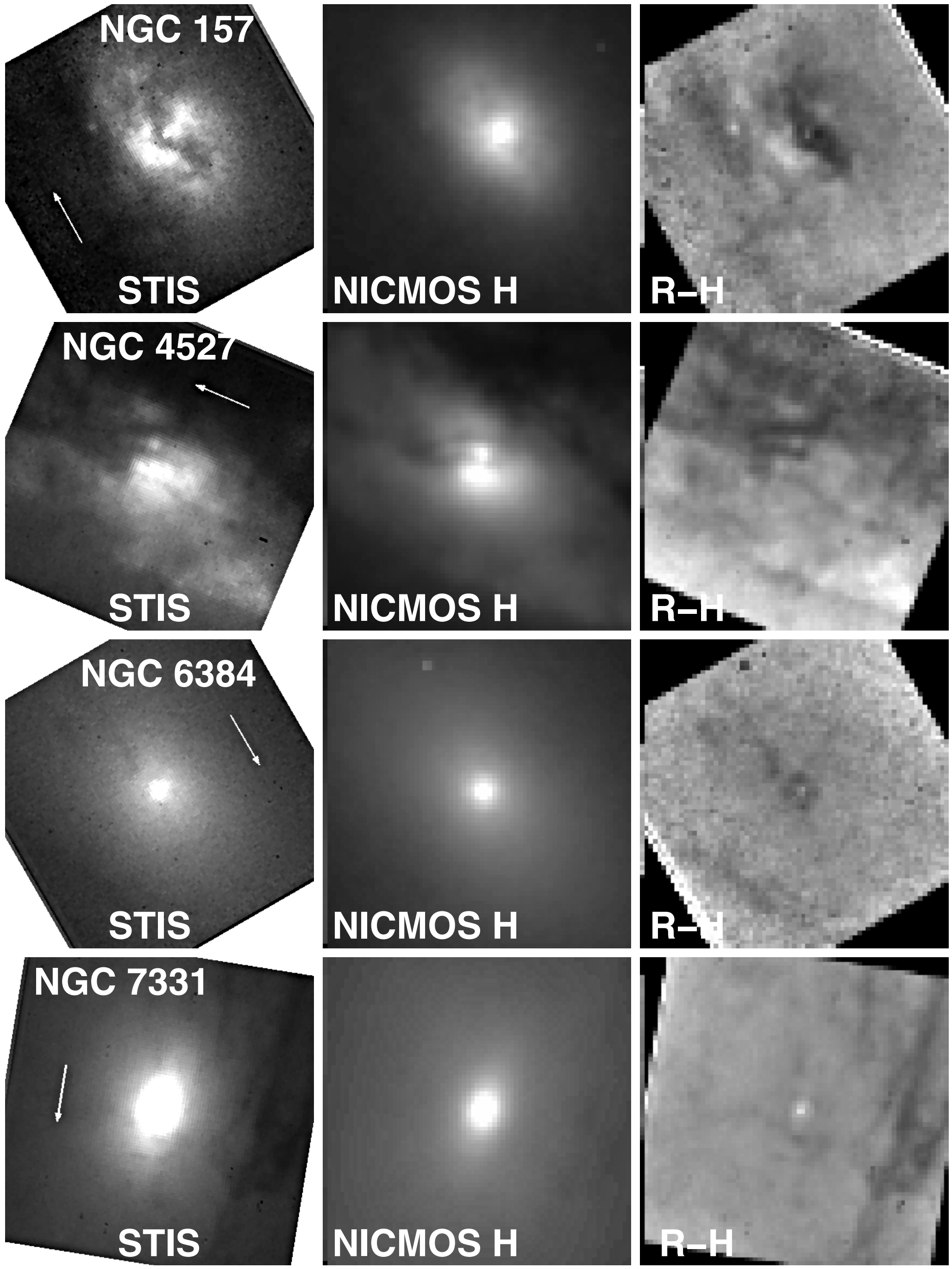

FIG. 19.—STIS images, NICMOS images, and the resultant color maps for galaxies with little or no emission lines in the spectra. The STIS spectra are approximately 5″ × 5″ before rotation. The images are rotated so that north is up and east is to the left. The white arrow on the STIS image indicates a scale of 1″ and the *y*-direction of the spectroscopic slits. The images have all been unsharp masked to enhance any structures present.

In this paper we present the successful STIS spectra from our massive black holes program. The emission lines in the spectra display a wide range of morphologies, and it is clear that most galaxy centers are affected by dust obscuration and/or lack of line emission, causing the spectra to appear patchy. These spectra are being used in our gas kinematical modeling to determine the central mass concentration in nearby spiral galaxies and to determine whether a massive black hole is present or not.

We would like to thank Andy Robinson for useful discussions. We have made use of the LEDA database (http://leda.univ-lyon1.fr).

REFERENCES

Alonso-Herrero, A., & Knapen, J. H. 2001, AJ, 122, 1350
Alonso-Herrero, A., Ryder, S. D., & Knapen, J. H. 2001, MNRAS, 322, 757
Axon, D. J., et al. 2003, in preparation
Barth, A. J., Sarzi, M., Rix, H., Ho, L. C., Filippenko, A. V., & Sargent, W. L. W. 2001, ApJ, 555, 685
Böker, T., Laine, S., van der Marel, R. P., Sarzi, M., Rix, H., Ho, L. C., & Shields, J. C. 2002, AJ, 123, 1389
Carollo, C. M., Stiavelli, M., de Zeeuw, P. T., & Mack, J. 1997, AJ, 114, 2366
Carollo, C. M., Stiavelli, M., de Zeeuw, P. T., Seigar, M., & Dejonghe, H. 2001, ApJ, 546, 216
Carollo, C. M., Stiavelli, M., & Mack, J. 1998, AJ, 116, 68
Carollo, C. M., Stiavelli, M., Seigar, M., de Zeeuw, P. T., & Dejonghe, H. 2002, AJ, 123, 159
Elmegreen, B. G., et al. 1998, ApJ, 503, L119
Elmegreen, D. M., Chromey, F. R., McGrath, E. J., & Ostenson, J. M. 2002, AJ, 123, 1381
Ferrarese, L., & Merritt, D. 2000, ApJ, 539, L9
Ford, H. C., et al. 1994, ApJ, 435, L27
Gebhardt, K., et al. 2000, ApJ, 539, L13
Graham, A. W., Erwin, P., Caon, N., & Trujillo, I. 2001, ApJ, 563, L11
———. 2002, preprint (astro-ph/0206248)
Ho, L. C., Filippenko, A. V., & Sargent, W. L. W. 1997, ApJS, 112, 315
Hughes, M. A., et al. 2003, in preparation (Paper III)
Hummel, E., & Jorsater, S. 1992, A&A, 261, 85
Kormendy, J., & Richstone, D. 1995, ARA&A, 33, 581
Laine, S., Knapen, J. H., Pérez-Ramírez, D., Englmaier, P., & Matthias, M. 2001, MNRAS, 324, 891
Macchetto, F., Marconi, A., Axon, D. J., Capetti, A., Sparks, W., & Crane, P. 1997, ApJ, 489, 579
Maciejewski, W., Teuben, P. J., Sparke, L. S., & Stone, J. M. 2002, MNRAS, 329, 502
Marconi, A., & Hunt, L. K. 2003, ApJ, 589, L21
Marconi, A., et al. 2003, ApJ, 586, 868 (Paper I)
Martini, P., & Pogge, R. W. 1999, AJ, 118, 2646
Martini, P., Regan, M. W., Mulchaey, J. S., & Pogge, R. W. 2003, ApJS, 146, 353
McLeod, B. A. 1997, in The 1997 *HST* Calibration Workshop, with a New Generation of Instruments, ed. S. Casertano, R. Jedrzejewski, C. D. Keyes, & M. Stevens (Baltimore : STScI), 281
Merritt, D., & Ferrarese, L. 2001, ApJ, 547, 140
Pérez, E., Márquez, I., Marrero, I., Durret, F., González Delgado, R. M., Masegosa, J., Maza, J., & Moles, M. 2000, A&A, 353, 893
Pogge, R. W., & Martini, P. 2002, ApJ, 569, 624
Regan, M. W., & Mulchaey, J. S. 1999, AJ, 117, 2676
Scarlata, C., et al. 2003, in preparation (Paper IV)
Schödel, R., et al. 2002, Nature, 419, 694
Seigar, M., Carollo, C. M., Stiavelli, M., de Zeeuw, P. T., & Dejonghe, H. 2002, AJ, 123, 184